Active Power Filters for Harmonic Mitigation in Power Systems

by

Riashad Siddique

B.Sc.E., Shahjalal University of Science and Technology, 2015

A Thesis Submitted in Partial Fulfilment of
the Requirements for the Degree of

Master of Science in Engineering

In the Graduate Academic Unit of Electrical and Computer Engineering

Supervisor: Julian Meng, Ph.D., Electrical and Computer Engineering

Examining Board: Yevgen Biletskiy, Ph.D., Electrical and Computer Engineering
Scott Bateman, Ph.D., Computer Science

This thesis is accepted by the
Dean of Graduate Studies

THE UNIVERSITY OF NEW BRUNSWICK

August, 2023

Abstract

The use of power electronics in all types of industrial, commercial, and residential loads can cause system-wide reduction of the power quality from harmonic distortion of the AC waveform. Residential non-linear loads resulting from heavily used power electronic devices and renewable energy sources at the distribution power system level can significantly contribute to harmonic distortion. With excessive harmonic distortion, traditional mitigation methods such as using passive filtering has had limited success. As such, this thesis aims to utilize active power filters to improve the distribution power quality affected by unwanted harmonic components. Various time and frequency domain harmonic detections methods are proposed and implemented in a shunt configuration topology. The goal is to assess active filtering techniques based on previously published research with novel modifications to improve performance based on harmonic reduction and convergence speed (settling time) in time-varying conditions.

Dedication

To the Almighty Allah and my beloved wife

Acknowledgements

I would like to thank my supervisor Dr. Julian Meng for his unconditional support and continuous encouragement during my study at the university and for the internship opportunity. I am heartily thankful to him for his deep concern towards my academics and for providing constructive guidance. This research would not have been possible without him.

Thanks are extended to my friends in the Smart Grid Lab, who made the period of my research a pleasant experience to cheer. I am thankful to the University of New Brunswick and the New Brunswick Innovation Foundation (NBIF) for all the funding regarding the project, which provided the opportunity to conduct this research.

Table of Contents

Vita

List of Tables

List of Figures

List of Nomenclature or Abbreviations

AC	Alternating Current
APF	Active Power Filter
DC	Direct Current
DFT	Discrete Fourier Transform
DSP	Digital Signal Processing
D	Direct
D-Q	Direct-Quadrature
FD	Frequency Domain
FDHD	Frequency Domain Harmonic Detection
FFT	Fast Fourier Transform
FT	Fourier Transform
HD	Harmonic Detection
HPF	High Pass Filter
IFFT	Inverse Fast Fourier Transform
LMS	Least Mean Square
LPF	Low Pass Filter
OSC	Oscillator
PCC	Point of Common Coupling
PLL	Phase Locked Loop
P-Q	Instantaneous Reactive Power
Q	Quadrature

SAPF	Shunt Active Power Filter
SDFT	Sliding Domain Fourier Transform
SHE	Selective Harmonic Elimination
TD	Time Domain
TDD	Total Demand Distortion
TDHD	Time Domain Harmonic Detection
$TDHD_1$	Time Domain Harmonic Detection 1
$TDHD_2$	Time Domain Harmonic Detection 2
THD	Total Harmonic Distortion
VSD	Variable Speed Drive

Chapter 1

Introduction

An ideal electrical distribution system consists of sinusoidal voltage and current waveforms with constant fundamental frequency and voltage magnitude. Ideal waveforms result in a highly efficient power system in terms of power generation, power transfer, and load operation. The possibility of these ideal conditions is rather limited given that certain devices and conditions may introduce undesirable harmonic distortion in both current and voltage waveforms [1]. Common devices include industrial/residential power converters, variable motor drives, magnetically saturated machines, switched mode power supplies, lighting controls, etc., contribute to harmonics resulting in power quality issues. Along with heating losses, important protection system devices can be affected by harmonic interferences and affecting the tripping current levels [2]. Such failures can lead to considerable damage to the power systems. Interestingly, devices that contribute to harmonic distortion are also affected by harmonics from other devices. This cyclical relationship indicates the importance of preventing harmonics from propagating throughout the grid.

Harmonics in the power distribution are defined as integer multiples of the fundamental or nominal frequency. For example, if the fundamental frequency is 60 Hz, then the 5^{th} harmonic is 300 Hz (5×60 Hz). The deviation from this perfect sinusoidal is represented by non-zero harmonic components having a frequency integer multiple of the fundamental frequency. Harmonic-related problems in the power systems arise due to the presence of the following [3]:

1) Non-linear loads defined by a time-varying impedance;

2) Phase imbalance in 3-phase systems;

3) High input voltage or current causing saturation effects;

4) Resonance from resistor (R), inductor (L) and capacitor (C) components.

Non-linear loads are one of the primary sources of harmonics in electrical power systems. They draw current discontinuously in short pulses, and their impedance varies throughout the fundamental period [4]. Diode rectifiers and switch-mode converters are a few of the well-known non-linear loads. As expected, the significant increase in the use of such power electronic devices contributes to harmonics in the electrical distribution. The harmonic content of the grid is also changing due to the recent rise of Distributed Energy Resources (DERs). Power converters used by such systems can introduce significant harmonics into the grid and the nominal grid frequency can become prone to frequency variations due to the intermittent nature, i.e. irregular characteristic of renewable energy resources. Given this concern, it is essential to try to reduce harmonic levels using various technologies at our disposal.

A basic approach of using passive RLC filters had limited success, given their inherent static design parameters. Alternatively, Active Power Filters (APFs) utilize Harmonic Detection (HD) techniques to dynamically estimate and track the fundamental frequency component using the distorted line current as the input. The HD process then uses an estimation algorithm to generate a reference waveform that represents the unwanted harmonic content. Power converters compatible with the APF design are then used to create the required harmonic compensation current to be added 180° out-of-phase at the filter connection or Point of Common Coupling (PCC). As expected, the APF performance is boosted by fast and accurate tracking of the fundamental component in dynamic situations [5].

Harmonic reduction and convergence speed (i.e. settling time) are vital for any real-time applications of this technology and, thus, will be thoroughly assessed for

various HD techniques for a shunt APF configuration. The main research focus of this thesis is to implement and test each APF variation under difficult harmonic conditions..

1.1 Background

Electrical power quality has become a significant issue for all industrial and residential customers. As stated previously, the wide use of non-linear power electronics for economical solutions to electrical power usage has led to substantial harmonic distortion to an unacceptable level for optimal operation. Depending on the non-linear load characteristic, the grid might be injected with positive or negative sequence harmonics. In short, the positive sequence harmonics rotate in the same direction as the fundamental frequency, but the negative sequence harmonics do not. Due to this phase change, ubiquitous AC motors will induce torque outside their operational mode. The individual effect of the loads on the harmonic content can be insignificant, but their collective contribution can affect the whole distribution system [6]. Besides waveform distortion, harmonics can also cause a drop in power factors and energy efficiency of the power systems, motors, and generators [7]. The distortion power due to the presence of harmonics can be defined as [8]

$$D^2 = S^2 - \left(P^2 + Q^2\right) \tag{1.1}$$

where D is the distortion power, S is the apparent power, P is the real power, and Q is the reactive power. The distortion power results in greater heat generation, reduced system efficiency, and developed torque in motors [9]. Also, supply current harmonics increase the transformer's copper loss, and voltage harmonics increase the iron core loss leading to a reduction in the efficiency of a transformer [7].

Harmonic pollution is one of the major leading causes that degrade electrical

power quality over time. An investigation by the Canadian Electrical Association showed substantial economic losses are related to power quality degradation due to injected harmonics [10]. Power lines are affected due to the increased I^2R loss, and power electronics equipment has a higher chance of malfunction since the zero crossing of the AC waveform may shift due to added harmonics. It may also cause detrimental effects on the control circuit operations for industrial applications such as motor drives and AC/DC power converters. Relays and other instrumentation can malfunction due to the presence of harmonics, which can bring the whole power system to a shutdown with extensive equipment damage [11].

To mitigate the harmonic issue, the standards IEEE 519-2014 and IEC 610 003-25 are commonly used [7]. Both standards have limits for current and voltage harmonics on the PCC at the distribution feeders. The harmonic content of the waveform is defined by the term Total Harmonic Distortion (THD), which is implied in both current and voltage harmonics.

For current, the THD is defined as:

$$\begin{aligned} I_{THD} &= \frac{1}{I_1}\sqrt{\sum_{n=2}^{n_{max}} I_n^2} \\ &= \sqrt{\left(\frac{I_{rms}}{I_1}\right)^2 - 1} \end{aligned} \tag{1.2}$$

where I_n represents the n^{th} order harmonics, I_{rms} represents the RMS value of the complete harmonic current, and I_1 represents only the fundamental RMS current magnitude. A similar equation also represents voltage THD:

$$V_{THD} = \frac{1}{V_1}\sqrt{\sum_{n=2}^{n_{max}} V_n^2} = \sqrt{\left(\frac{V_{rms}}{V_1}\right)^2 - 1} \tag{1.3}$$

where V_n represents the n^{th} order harmonics, V_{rms} represents the RMS value of the complete harmonic voltage, and V_1 represents only the fundamental RMS voltage magnitude. The IEEE 519 harmonic limits are based on the ratio of short circuit current, I_{SC} to the fundamental component of the load current, I_{L1} at the PCC. This ratio is termed short circuit ratio, I_{SC}/I_{L1}. The harmonic limits for general distribution systems at voltages of 120 V to 69 kV are given in the table 1.1.

Table 1.1: IEEE 519 Harmonics Limit for 120 V to 69 kV Distribution Systems

I_{SC}/I_{L1}	$n < 11$	$11 \leq n \leq 17$	$17 \leq n \leq 23$	$23 \leq n \leq 35$	$35 \leq n$	TDD
< 20	4%	2%	1.5%	0.6%	0.3%	5%
20-50	7%	3.5%	2.5%	1%	0.3%	8%
50-100	10%	4.5%	4%	1.5%	0.7%	12%
100-1000	12%	5.5%	5%	2%	1%	15%
> 1000	15%	7%	6%	2.5%	1.4%	20%

The term TDD is defined as Total Demand Distortion. For non-linear loads, under light load conditions, THD values can be misleading as it represents the harmonic percentage based on the instantaneous fundamental current. If the fundamental current is low, harmonic current may be significantly low. This insignificant current may not cause any serious harmonic deterioration in the power grid but the THD value in this case will misrepresent the harmonic influence. To avoid this scenario, IEEE

introduced TDD expressed as,

$$I_{TDD} = \frac{\sqrt{\sum_{n=2}^{n_{max}} I_n^2}}{I_{\text{rms1}}} \tag{1.4}$$

where I_{rms1} represents the RMS magnitude of the rated fundamental load current at the PCC. During light load conditions, the harmonic current may be significant compared to the instantaneous fundamental current but may be insignificant compared to the rated fundamental load current at the PCC.

1.2 Literature Review

Passive filters were initially employed to mitigate the harmonics in the electrical supply. They act as harmonic sinks and provide a low-impedance path for the harmonic currents to travel into the ground. Most of the harmonics originated from industrial loads in the early grid infrastructure, and the utilities usually installed passive filters to reduce harmonic content on the generation side. Aside from the modern system-wide distribution of harmonic loads, the tuning frequency changes over time, primarily due to capacitor aging and grid expansion [1]. As a result, component aging or a change in the grid setup must follow with a corresponding change in the filtering application.

Controlling the harmonic pollution using the passive filters can also unintentionally generate additional resonance, which could lead to the failure of these filters [12]. Due to the power system dynamics, variation in the tuning frequency, and random characteristics of load harmonics, APF is considered in this research for harmonic mitigation and suppression [13]. In real-time applications of APFs, HD methods are implemented using Digital Signal Processing (DSP) technologies to estimate a

reasonable approximation of the harmonic waveform. As expected, any errors in the HD estimation process will reduce the effectiveness of the APF as the residual harmonic content can still be significant to generate notable harmonic distortion [14]. Overall, the successful mitigation of the harmonic using APFs will highly depend on the accurate estimation of the fundamental wave parameters (i.e., amplitude, frequency, and phase) from which the residual harmonic waveform can be estimated. Only then the harmonic compensating current generated by the APF will closely reflect the harmonic distortion present at the line level. For this research, various HD methods will be integrated into one of the selected APF topologies described in chapter 3. In the early APF implementation, only harmonic currents were used as reference signals for detecting distortion. However, accurate estimation of the fundamental waveform parameters using only distorted line currents is problematic with the added difficulty of any variation in the fundamental period [15].

Since the current distortion also contributes to the voltage distortion, the voltage signal cannot be considered to determine the parameters of the fundamental period. As a result, the voltage THD can still be above the IEEE limits, and the electrical grid is not truly free of harmonics. More recent applications of HD utilize Phase-Locked Loop (PLL), which proved beneficial to overcoming the voltage distortion and frequency tracking issue. The PLL accurately tracks both the amplitude and phase of the fundamental frequency component, thereby making the HD process more robust.

HD methodologies are primarily divided into two categories: Frequency Domain (FD) and Time Domain (TD) based methods [16]. Relative strengths and weaknesses of processing signals in either domain are based on the computational requirements and flexibility. The harmonic calculation required by the APF can generate phase delay (or time delay) between the compensation current and the line harmonics [14]. Phase delays are unavoidable for causal systems but should be as low as possible to

ensure the estimated harmonic waveform from the HD output aligns as closely as possible with the distorted input. Both frequency tracking capabilities and the phase delays will impact the design constraints of the APF.

The mathematical model of each domain-specific HD method is presented in [16] and are summarized based on their processing domain. Frequency domain HD (FDHD) methods are mainly implemented using the Discrete Fourier Transform (DFT). The electrical signal in TD is converted to FD, and the unwanted harmonic components can be identified by extracting the amplitude and phase of the fundamental frequency component. A major drawback of Fourier analysis is repeating the discrete sampling requirement over each period with the added burden of the DFT. Advantages include the ability to estimate the magnitude and phase values of desired frequency components with improved robustness to noise. Earlier FD methods achieved limited success due to harmonically distorted signals requiring a longer common period to resolve the frequency components [17]. The resulting DSP computational burden contributes to added phase delays, which can ultimately degrade the APF performance.

Time Domain HD (TDHD) methods do not require the computational burden of translating voltage and current signals into the FD for processing [18] and can avoid fixed-length input processing of the sampled signal. TDHD methods use a transformation matrix to estimate the fundamental frequency component from a 3-phase harmonically distorted system. This process is noise resistant and can significantly improve the robustness of the APF. For this category of APFs, authors in [19-22] developed Selective Harmonic Elimination (SHE) method that can be used even in unbalanced conditions. Further developments in the TDHD methodologies can be seen in [23-25] with the introduction of adaptive filtering techniques to estimate and track the fundamental frequency component of a harmonically distorted sinusoidal signal. The distorted portion of the signal can be considered as a residual or noise

component needed to be removed. The adaptive TD techniques rely on their convergence properties and have the ability to self-tune to slight variations in the nominal frequency.

Unwanted harmonics will deviate the AC sinusoidal signal's natural zero crossing and affect power converters that require a non-distorted AC source for operation. Also, DSP-induced errors such as aliasing, leakage, and picket fence effect are common when calculating the harmonics by steady frequency estimation [26]. Aliasing is a well-known consequence of Shannon's sampling theorem, and leakage refers to the apparent spreading of energy from one sampled frequency into adjacent ones due to frequency deviation, which may reduce the nominal frequency resolution to unacceptable levels. Picket-fence effect can be observed if the analyzed signal includes a frequency that is not an integer harmonic frequency of the fundamental.

This research will implement two TDHD methods described in subsection 3.3.1 and subsection 3.3.2. The latter can be considered an advancement in TDHD with enhanced power quality and improved harmonic reduction. A FDHD method based on efficient data management via the DFT process is implemented for comparison purposes. The harmonic suppression performance depends on the HD accuracy and provides the foundation of the APF operation. The harmonic distortion will continue to rise with the increased commonality of the non-linear loads and DERs and the APF must be capable of adapting to changing infrastructure and the resulting harmonic conditions.

1.3 Thesis Objectives and Contributions

A major goal of this thesis is to test the APF using various HD methods under changing load and grid conditions. The APF performance will be evaluated based on the following characteristics:

1) Ability to track changes in the nominal frequency
2) Harmonic mitigation capabilities in steady-state conditions.
3) Settling time duration in response to dynamic changes.

The selected HD method is instrumental in determining how well the APF manages under difficult harmonic conditions. The first TDHD method ($TDHD_1$) is based on a Direct-Quadrature transformation and is an established approach to extract the fundamental component from the distorted load current. A significant drawback of the $TDHD_1$ is the additional phase delay due to the required interdomain transformations. The second TDHD method, ($TDHD_2$) is based on a Least Mean Square (LMS) adaptive filtering approach that can self-tune under changing load conditions and can be implemented using sample-by-sample processing. Adaptive techniques require careful consideration on the selected prediction algorithm as this dictates the tracking ability of the filter (e.g., settling time and steady-state error) [27]. The final HD method is a FD approach based on a computationally efficient variation of the DFT resulting in a minimal phase delay. Earlier FD methods behaved poorly in the presence of changing load conditions as the periodicity of the signals was lost and fixed-length data inputs limits time resolution to dynamic changes. Our implementation utilizes the Sliding-Domain Fourier Transform (SDFT) method to process the input signal sample-by-sample, improving computationally efficiency compared to the DFT. Although all HD techniques have their strengths and weaknesses, it is the main goal of the selected HD method to estimate the fundamental waveform as quickly and accurately as possible. This is the key to the APF performance.

Chapter 3 provides background information on basic passive and active filter implementation as well as a detailed analysis of the three proposed HD techniques. Some improvements to these HD methods include limiting interdomain transformations, and sampling requirements are presented to achieve better transient, and steady-state performance. Simulation and test results are given in chapter 4.

1.4 Thesis Structure

The organization of the thesis is as follows, chapter 2 reviews the overall process of harmonic build-up in a modern distribution system. The main characteristics of the distribution feeders that affect the harmonic situation are discussed. The chapter addresses the power quality issues affected by harmonic pollution due to the emergence of renewables and the corresponding factors to have the APF for harmonic mitigation.

Chapter 3 introduces the three HD algorithms: $TDHD_1$, $TDHD_2$ and SDFT used in APF applications. The chapter will thoroughly review each of the HD mentioned earlier. It should be noted that $TDHD_1$ algorithm is well recognized for its HD capabilities and will be used as baseline reference for comparison purposes. Some interesting features in our implementation of these three HD techniques include:

- ▷ The predictive control algorithm used in $TDHD_2$ utilizes a variable convergence coefficient step size to considerably improve frequency tracking and settling time.
- ▷ Unlike the previous algorithms of active filtering, the Park's transformation matrix used in our implementation of $TDHD_1$ determines the reference current for error calculation. This is an upgrade to previous APF applications based on a transformation matrix that does not have this capability [28].
- ▷ The SDFT HD method is a substantial upgrade compared to the earlier DFT methods due to reduced calculations.

Chapter 4 will provide the simulation and performance results of the TDHD and FDHD methods explored for this research work. The results will consist of a comparison study of settling time and harmonic reduction capabilities in various harmonic conditions. Chapter 5 provides a summary of the research outcomes of this thesis and some future work associated with the proposed HD techniques.

Chapter 2

Modern Distribution Systems and Harmonics

2.1 Harmonic Sources

An electrical distribution system is a complex dynamic system that usually suffers from unexpected current and voltage waveform changes contributing to harmonic distortions. The harmonic distortions can occur due to the increased usage of non-linear loads such as solid-state electronic devices (e.g. power converters, switched-mode power supplies, etc.), along with more conventional causes such as magnetic saturation of a transformer and highly inductive loads in heavy industrial applications [29].

The associated harmonic distortion of the transformer depends on the design and operation of this device. During significant disturbances due to electrical power surges or no-load conditions, the transformer can increase the overall harmonic content of the grid from core saturation effects. Core saturation occurs most when the transformer operates above rated power or below the rated voltage. The first situation can arise during peak demands, and the second in light load conditions, particularly at night. If the transformers are operated in the saturation region, they exhibit non-linear magnetizing currents consisting mainly 3^{rd} order harmonic distortion [30]. The step-up transformers connecting the generation plant to high-voltage transmission lines are most prone to harmonic effects due to this saturation zone of

the transformers. Transformer harmonic solutions include using Delta-Wye connections to manage harmonics and prevent the distorting waves from traveling back to the generators [31].

Rotating electric machines are designed to have a perfect sinusoidal distribution of magnetic flux around their air gap so that the device is not operated in the saturation region. The perfect sinusoidal magnetic flux distribution is hard to maintain in salient pole structures. Due to this inherent imperfection of the magnetic flux, saturation can result causing rotating machines generating harmonics similar to transformers.

Arc ignitions have non-linear voltage characteristics. Voltage variations due to the sudden alterations of arcs alone can produce a wide spectrum of non-fundamental frequencies. The effects are more pertinent during the melting of the scarps and the refining process. Luminous discharges are highly non-linear and give rise to multiple odd harmonics in the system. The dominant 3^{rd} harmonic produced by such lighting devices travels in the neutral wire of the 3-phase system. The magnetic ballasts installed in the fluorescent lamp contain magnetic core inductors to limit the current in the tube. The non-linear characteristics of the magnetic ballasts will introduce excess harmonics in the system.

Non-linear loads have also dramatically changed the residential harmonic signature; computer power supplies, AC/DC power converters, etc., now exist in every modern home and office. Although an individual household's harmonic magnitude is generally substantially less than the industrial harmonic output, the problem becomes more pronounced when harmonics are aggregated at low-voltage distribution transformers. Residential harmonic signals can superimpose, and their total magnitude can be compared with their industrial counterpart.

Apart from load harmonics, integrating DERs also makes the harmonic signature more unpredictable. DERs like Photovoltaic Cells (PVs) and wind turbines are

extensively dependent on weather conditions and the utilization of power converters for grid connections. According to [30, 32] residential sector in the North American grid will experience a significant increase of solar power in the foreseeable future and could increase further due to the falling prices of installation costs. In the meantime, wind power will grow to 11% by the year 2040 and will also contribute to harmonic frequencies on the grid due to AC/DC power conversion processes.

The preliminary step in planning an effective harmonic mitigation strategy is having an accurate model of the harmonic source. This chapter discusses these phenomena and is organized as follows:

- ▷ Section 2.1 describes the harmonic sources;
- ▷ Section 2.2 focuses on the harmonic effects;
- ▷ Section 2.3 discusses the impact of harmonics on power quality and the importance of harmonic mitigation;
- ▷ Section 2.4 illustrates the build-up of harmonics in the power grid;
- ▷ Section 2.5 establishes the objectives and the methodologies for the harmonic source models described in [33, 34].

As stated earlier, non-linear devices in residential and commercial settings are critical sources for harmonics in the grid. However, it is difficult to identify the responsible load from the distorting harmonic spectra at the utility end. A more flexible method for simulating harmonic distortion at the distribution level is described in section 2.5. The harmonic model implemented in this chapter will be incorporated into a load aggregation at the residential level, and this avoids the need to identify the location of individual harmonic loads in the distribution systems. Also, in doing so, an unbiased view of the device's harmonic contribution to the grid is achieved as various harmonic types are blended. For a stable and efficient distribution system operation, it is important to understand the nature of the harmonics and to track the nominal frequency for successful harmonic elimination [35]. For this thesis, the

harmonic build-up at the distribution level from the industrial and residential loads is based on [33, 34]. A residential distribution and feeder system is simulated and will be used extensively to evaluate the APF performance.

2.2 Harmonic Effects

As stated earlier, the harmonic signals from the low-voltage sides merge into the primary feeder through the distribution transformers. Harmonics cause deviation of the voltage and current signal from their usual mode of operation and can cause the protection equipment to malfunction. Overheating of conductors, reduced efficiency, and longevity of electrical equipment are common phenomena that arise due to frequent harmonic issues [36]. The following is a summary of the harmonic effects.

1) **Distribution transformers**

   Earlier, it was discussed that over-driven transformers could be a source of harmonics. However, they can also be affected by the presence of harmonics created from other sources. In a distribution transformer, harmonics can cause an increase in copper and stray flux losses. Compared with a pure sinusoidal current, the propagating harmonic current from the applied source can lead to a higher temperature weakening the thermal protection and the eventual tripping of the Buchholz relay, which is installed to protect the transformer from fault current. In addition, harmonics cause additional eddy current losses in the transformer, which reduces the efficiency and may lead to blown-out fuses due to excessive heating [36]. There also exists the possibility of resonance between the transformer inductance and the line capacitance due to unwanted harmonic.

2) **Electric cables**

   Harmonic currents of higher order inside the electrical conductors can result in

increased heating due to skin and proximity effects when compared to fundamental current. Both effects depend on frequency as well as the size and shape of the conductor and increase the equivalent AC resistance, which in turn leads to increased I^2R_{AC} loss [37]. Dielectric breakdown of the cable insulation can occur due to the harmonic overvoltage of the system [36].

3) **Rotating machines**

Rotating machines like generators and motors can also be negatively affected by unwanted harmonics, and these machines can undergo similar thermal effects to transformers. As the resistance of the conductor increases due to an increase in frequency due to the skin effect, supply currents rich in harmonics will cause greater heating of the machine. In addition to the thermal effects, the positive and negative sequence harmonics can create pulsating torques [36,38]. This occurs as positive sequence harmonics aid the machine's torque while negative sequence harmonics have the reverse effect. Pulsating torques have undesired effects on the shafts of the rotating machines, including equipment fatigue, increased vibration, and bearing wear out [30]. Also, negative sequence harmonics in the generator can cause severe overheating in the rotor circuit, which may eventually melt or damage the rotor control circuit [8].

4) **Protection, communication and electronic equipment**

Harmonics can affect metering devices, protection equipment, and communication circuits in electrical distribution networks. Harmonics can interfere with the interruption capability of the circuit breakers, relays whose operations are a function of the peak voltage/current [7]. Even the time delay characteristics of the electromagnetic-type relays will be altered in the presence of harmonics. The ground relays can cause erroneous tripping as they cannot distinguish between the zero sequence and third harmonic currents [1]. Due to inductive coupling, harmonics can interfere with the telephone lines and may also shift

the zero crossing of the sinusoidal signals resulting in an impaired operation of the electronic and control circuits.

5) **Power factor correction capacitors**

It is well known that a capacitor's reactance decreases with increasing frequency, and therefore the capacitor acts as a sink for harmonic signals. This effect increases the heating and dielectric stress of its insulation material. The presence of voltage distortion increases the dielectric loss of capacitors expressed by $\sum_{n=1}^{\infty} C\left(\tan\delta\right)\omega_n V_n^2$, due to the frequency-dependent loss factor $\tan\delta = R\omega_n C$ where $\omega_n = 2\pi f_n$ and V_n is the RMS voltage of the harmonic order n [39]. The increased heating and voltage stress due to harmonics reduces the life of power factor correction capacitors. Eventually results in the dielectric breakdown of the capacitor [36].

The control of the nominal frequency is an essential part of the power system operations. Imbalances between load and power generations need to be solved in seconds to avoid frequency deviation from their nominal values to ensure the stability of the power system. These common variations are managed by the governor of the generation units known as primary frequency response; one of the three responses available for the conventional generation units [40]. This frequency control reserve power is available to compensate for the drop in frequency in any instant.

Due to the increasing energy demand and desire for clean energy, the importance of DER is becoming more important as they have a minimal carbon footprint. Increased penetration of renewable energy sources has increased the frequency deviation and harmonic issues [41]. For example, intense fluctuations in the minute range have been observed from the wind farms by West Danish power systems due to unstable weather conditions [42]. A change in the power injection by the wind system can deviate the grid frequency from the nominal value and introduce harmonic frequencies to the grid. It is important to estimate harmonic content as quickly and

accurately as possible, given the harmonic sensitivity of protection devices and other various machines connected to the grid. Therefore, harmonic filters are crucial for power systems operators to maintain the power quality to utility standards.

2.3 Harmonic Mitigation Strategies

Harmonic studies on electrical networks have been carried out since early 1916 due to the saturation of the transformer cores. It is evident from the previous sections that harmonics lead to various disturbances in the electrical network. There are two primary options to deal with harmonic pollution from studies conducted in the past, active and passive treatment [43]. One solution for an active treatment is the utilization of power electronic devices with high power factors to reduce the imbalance between the phases so that the harmonics originating from phase imbalances can be reduced. However, this method is not efficient in controlling harmonic pollution of other variants.

Depending on the nature of the grid dynamics, passive or active harmonic filters can also be used to filter out non-fundamental frequencies. Both filtering methods have been proven effective in controlling harmonic distortion if the disturbances are within their operational capabilities. Passive filters fail with changes in grid impedance, network expansion of DERs, and aging of filter components, with the latter impacting the filter's original frequency response. Alternatively, active filters can operate successfully in these conditions, given their ability to dynamically track deviations in the nominal grid frequency for the purpose of removing unwanted harmonic content. These capabilities, however, require more complexity in design and implementation when compared to passive filter designs.

The shunt configuration of passive filters is widely used with DERs to divert the harmonic currents entering the grid. However, the passive filters need to be

properly tuned with tolerant values from ±3% to ±15% for the desired harmonic frequencies to mitigate. Even then, manufacturing errors and capacitors' temperature sensitivity often lead to tuning frequency deviation of the passive filters [44]. This unwanted deviation can result in harmonic voltage amplification, which may lead to poor power quality in the adjacent network. The effects will be prominent in the islanded operation mode. In analyzing these issues, passive filters may not be viable to mitigate future harmonic concerns.

The current grid structure is populated with increasing non-linear devices, and the passive filter is inefficient in keeping the harmonic levels within the defined threshold of IEEE 519-2014 [7], and IEC 1000-3-6 [45]. These harmonic standards are based on lumped harmonic sources where the industrial sections of the grid are the primary sources of harmonic disturbances. This philosophical assumption does not hold in the era of smart grids. The wide distribution of the harmonic loads makes them difficult to monitor and eliminate using passive filters. In analyzing these issues, passive filters are not viable to mitigate the harmonic concerns of current and future power systems. Alternately, research shows that APF can operate effectively under challenging harmonic situations, ensuring the power system operates with high reliability and stability. The following chapter provides a detailed discussion on both types of filter implementations.

2.4 Residential Distribution System

Figure 2.1 shows a typical residential feeder in the North American grid. The primary feeders transfer the electrical power from the substation to several distribution transformers. As mentioned in the previous chapter, residential loads were not initially considered for significant harmonic contribution to the power grid. With the advancement of consumer power electronics and higher levels of renewable energy

use, the harmonic origins are shifting more towards residential feeders than industrial feeders. This rising concern has increased the importance of studying the effects of harmonics from residential loads.

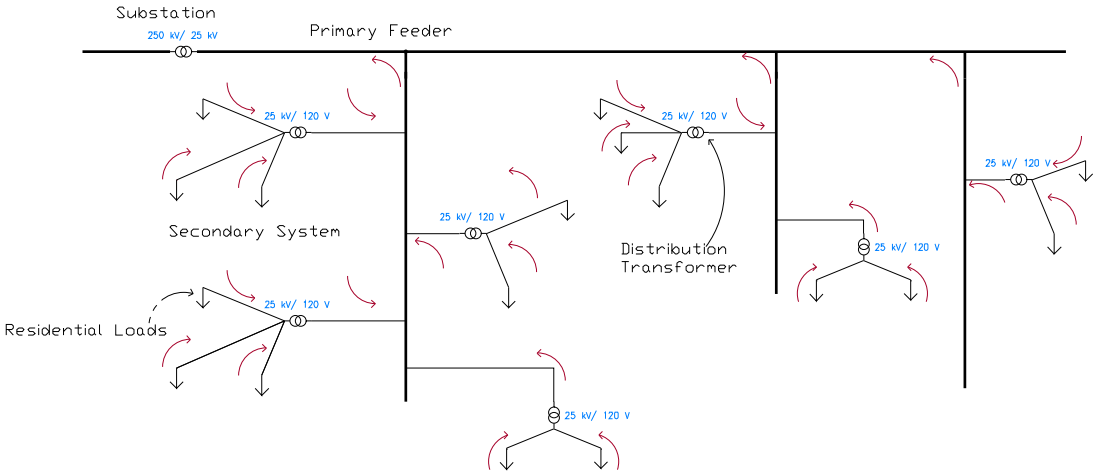

Figure 2.1: Schematic of a Residential Distribution Feeder in North America

As shown in the Figure 2.1, the houses are connected to 120 V side of the distribution transformers through the secondary conductors. Generic home appliances (compressors, power converters, lighting, etc.) are the primary harmonic sources in the system. As illustrated by the red arrows in the Figure 2.1, each residential customer injects harmonics into the system, penetrating the primary feeder and flowing toward the substation. As expected, an aggregation of residential units utilizing many power electronic devices can contribute significant harmonic distortions to the power quality. Figure 2.2 shows the harmonic build-up to the distribution transformers and the propagation of the harmonics to the substations.

The residential units are connected to the distribution transformer as shown in Figure 2.4 [46] in the next section. The standard secondary line structure is a 120 V or 240 V three-wire service. Each distribution transformer typically supplies 10 to 20 customers. The substation side of the distribution transformers can be an ideal location to install an APF and test the HD methods. APFs will help reduce the harmonic signals superimposed on the low voltage side before traveling up the

primary feeders to merge with the other harmonic signals from different parts of the grid.

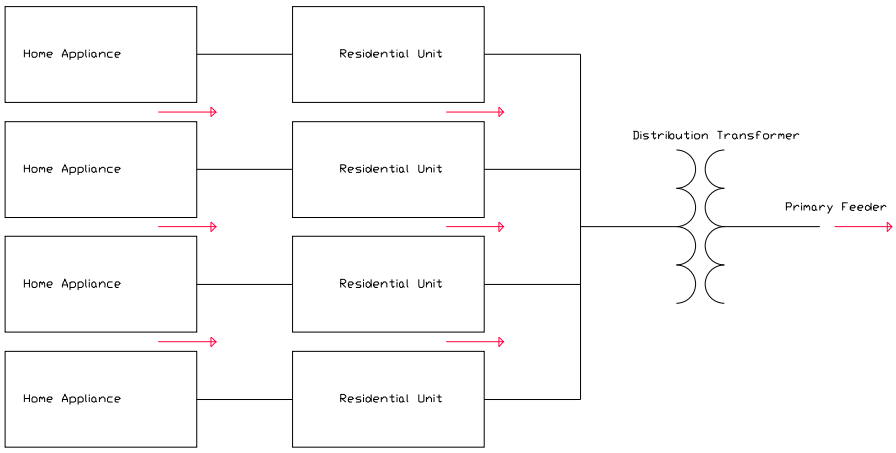

Figure 2.2: Harmonic Build Up Model

As countries prioritize their net-zero carbon reduction policies, DERs such as rooftop PVs will become more popular with residential customers. PVs are considered as dynamic systems as they depend on the weather and time of the day to produce power. The harmonic distortion from these panels depends on their generated power and the power conversion unit installed for home integration. Usually, the THD is high during low power output, which typically occurs with bad weather or dimming daylight [30]. The injection of harmonics from PVs results from using the common Pulse-Width Modulation (PWM) method for DC/AC conversion. In this technique, pulses used to form the AC waveform result in switching transients that introduce the undesired harmonics. In fact, any power conversion technique used in a DER system is also susceptible to this phenomenon. Electric Vehicles (EVs) will also have a similar effect as PVs, given the need for a power conversion unit for charging/discharging.

2.5 Residential Harmonic Source Modelling

A harmonic model at the distribution transformer level is needed to evaluate the impact of the non-linear residential loads on distribution systems. For the studies conducted in this thesis, the residential harmonic sources including the rooftop PVs are modeled employing the bottom-up probabilistic approach introduced in [33, 34]. The key idea is to combine the multi-residential harmonic models into one aggregated harmonic model, and this approach can be summarized by the following steps [34]:

1) The types of regularly used electrical home appliances are recognized.
2) The number of appliances per household is estimated.
3) Appliances are modeled as constant power loads in their rated operational frequency. Current sources are used to model the non-linear loads.
4) The individual harmonic models are combined to build an aggregated harmonic model for each home.
5) The residential units are connected to the secondary distribution transformer.

This chapter indicates some various load types that can generate residential harmonics but power converters are the main non-linear residential load type considered in this thesis. In the steady-state operation of power converters, the shape of current and voltage waveforms changes due to the converter action. This change affects AC and DC in action; the generated harmonics depend on the converter's pulse order. An equivalent model based on [47] is employed to reduce the complexity and computation time. Multi-phase PI models are used for the transmission and distribution lines in the feeder. A neutral wire is also included by employing the developed model in [47]. The model structure is shown in Figure 2.5 and consists of loads connected to 120 V to neutral, −120 V to neutral and between 120 V & −120 V. Appliances connected between the latter case (such as washing machines, refrigerators, dryers) are considered to have linear impedance and therefore are a non-harmonic produc-

ing source. The model allows us to combine each house in parallel to create the equivalent circuit of the following Figure 2.3.

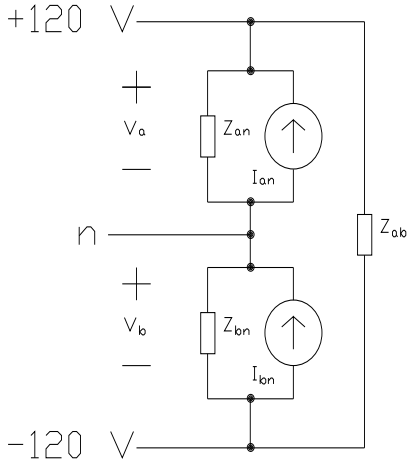

Figure 2.3: Bottom-up Residential Model

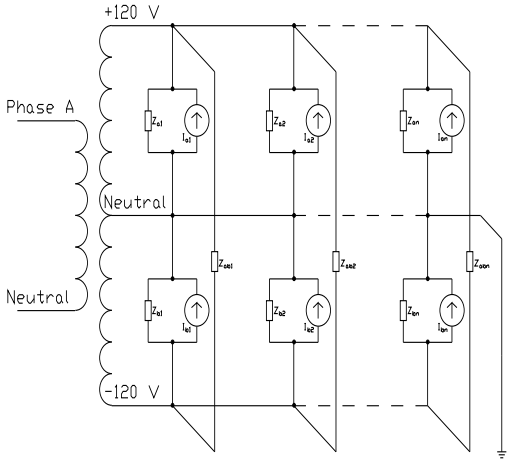

Figure 2.4: Multi-Residential Equivalent Model

Z_{ab} increases the complexity of the model; hence a new equivalent model for the branched load is developed in [48]. Z_{ab} is separated into two parts

Z_1 and Z_2 are in parallel with Z_{an} and Z_{bn} and are converted to ZT_1 and ZT_2 by parallel addition.

$$Z_1 = \frac{V_a}{V_a + V_b} \times Z_{ab} \tag{2.1}$$

$$Z_2 = \frac{V_b}{V_a + V_b} \times Z_{ab} \tag{2.2}$$

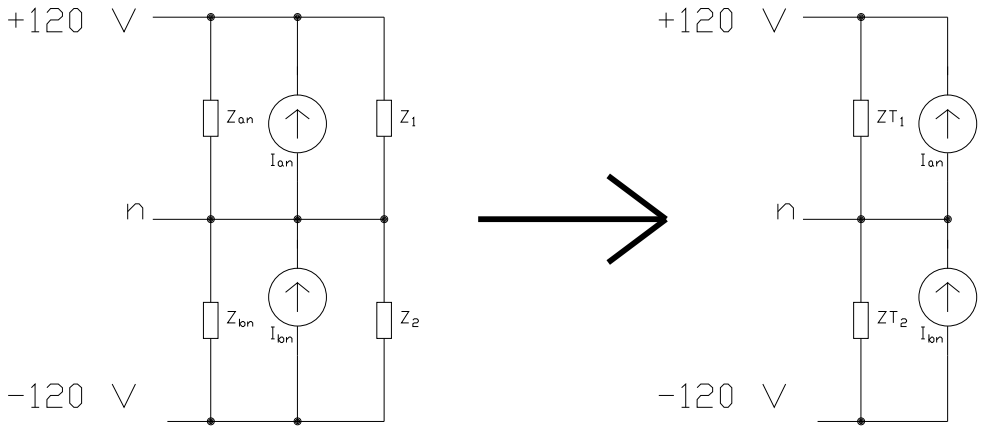

Figure 2.5: Final Equivalent Model of Single Phase Two Branch System

Finally, aggregated model of Figure 2.6 can approximate residential units connected to a single distribution transformer. By implementing the model developed in [48] Figure 2.7 simplifies the aggregated model.

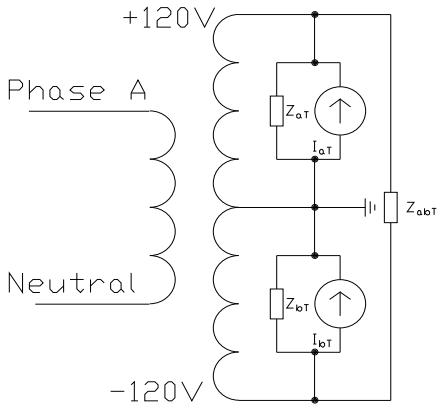

Figure 2.6: Aggregated Residential Units

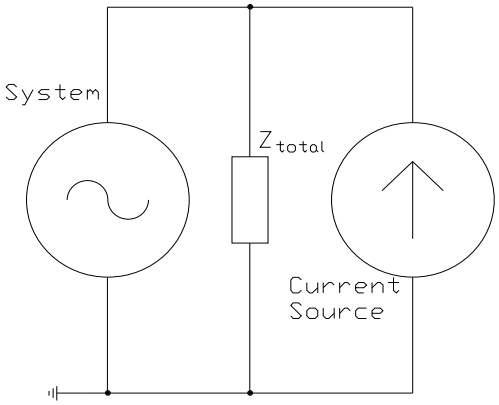

Figure 2.7: Simplified Aggregated Model

The connected linear appliance is paralleled as Z_{total}, and non-linear current sources are added as a new current source. Since the power electronic devices are individual bridge rectifiers, the AC signal is chopped off to produce the required DC waveform. This chopping action from the power electronic devices causes significant switching transients, which lead to the build of harmonics on the AC side. In other words, the harmonics signals are injected into the AC side. The reflected AC currents can be modeled as a current injection into the system. The PVs harmonic output signals have also been modeled in a similar fashion to incorporate into this research.

The residential load modeling provides a better understanding of harmonic effects on the distribution system. Proper modeling will map the voltage and current distortion due to the residential device impedance connected to the low-voltage side. This harmonic modeling will help us better understand the issues facing the distribution system at the residential level.

Chapter 3

Harmonic Filtering Methods

The importance of harmonic filters has been explored in Chapter 2 as they provide the necessary protection from the troublesome harmonic waveforms. Historically, passive harmonic filters were installed near the industrial plants as they were found to be the primary sources of harmonics in the grid. The recent emergence of household power electronics has resulted in great levels of harmonic distortion [49]. The ubiquity of consumer power electronic devices, along with more integration of DERs, different approaches are now being considered for harmonic compensating that are more distributed in nature. Modern DSP capabilities and power electronics allow for the development of smaller, more efficient, modular solutions to harmonic suppression.

This chapter introduces various passive and active harmonic filter implementations used to limit harmonic levels up to an acceptable magnitude. Section 3.1 illustrates various passive filters, and their working principles will be elaborated while highlighting their disadvantages in integrating with the modern power systems. Active filters and their different types will be discussed in section 3.2. In this section, the advantages of the APF over passive filters will be explained, and it describes why the APF is a better choice for solving the existing harmonic pollution on the modern grid.

In section 3.3, three types of HD methods used by the APF will be explored. The section will explore the specifics of the detection algorithms together with the advantages and disadvantages of each. Contemporary improvements made in the HD process are also discussed. In chapter 4, APFs based on these HD methods

have their performance accessed based on accuracy, convergence, and settling time response under difficult grid conditions.

3.1 Passive Filters

Passive filters are designed to bypass the harmonic signal or block them from entering the source side, with typical topologies shown in Figure 3.1, Figure 3.2, Figure 3.3, Figure 3.4 and Figure 3.5. The filters are implemented in series or shunt configuration, and the use of passive elements such as resistors, inductors, and capacitors (RLC) is the reason behind their simplistic made up.

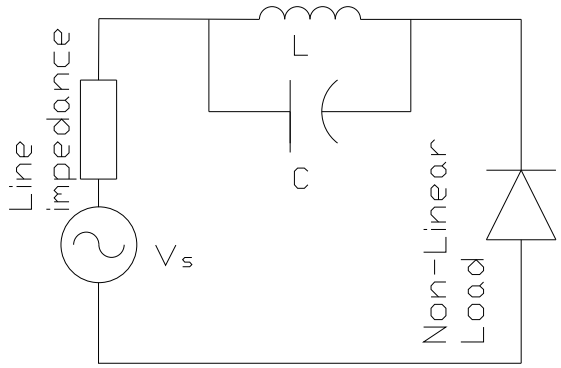

Figure 3.1: Series Passive Filter

The series configuration provides a high impedance path at its tuned frequency, preventing the flow of the harmonic current into the source side. The series passive filter is designed to carry rated full load current. Hence, it has the inherent risk of overload due to the excessive addition of the harmonic loads in the grid and may result in an increase to the grid THD level. The shunt configuration offers a low-impedance path for the harmonic current at its tuned frequency, and doing so diverts the harmonic current flow into the power source [50]. The shunt passive filter design includes the following network topologies:

1) **Single tuned filter**

This filter topology shown in Figure 3.2 has an RLC connected branch in parallel to the harmonic load. The passive elements in the RLC branch are chosen so that the filter impedance seen by the harmonic current is at a minimum near the resonant or harmonic (tuned) frequency. This low impedance path for selective order of harmonics can provide an alternate direction for the non-fundamental currents to flow. This change in the current path can help the distribution transformers to limit harmonic damage. The resistor is used to adjust the filter's tuning frequency and the effective bandwidth.

2) **First order filter**

The filter topology shown in Figure 3.3 falls into the High Pass Filter (HPF) family, which can remove frequencies higher than a certain magnitude. Above a certain threshold frequency, the RC branch can be low enough to divert the harmonic currents flowing into the grid. HPF filters can re-route the harmonic current flow only for higher frequencies, unlike the single-tuned filter. The resistor is chosen to limit the current flow through the capacitor and prevent thermal damage. Due to the nature of capacitive reactance, a large capacitance is required to achieve the desired low cut-off frequency. Since the HPF are installed between the line voltage and ground, the HPFs can act as unintentional compensating capacitors in low loading conditions [1]. If the grid is absent of harmonic current, a large thermal loss can happen due to the large impedance of the filters at the fundamental frequency.

3) **Second order filter**

This filter class shown in Figure 3.4 comprises a capacitor connected in series with a resistor and inductor connected parallel to each other. Below the cut-off frequency, it behaves closely to a single-tuned filter, while above the cut-off, it behaves as an HPF. The inductor causes the harmonics to bypass the resistor

at low frequencies and alternately bypasses the inductor at higher frequencies. The resulting has an attenuation of 40 dB/decade and allows for more flexibility in the design and requirements compared to the first order filter.

4) **Third order filter**

The passive filter implementation shown in Figure 3.5 has the same characteristics as the second-order filters, except it has an attenuation of 60 dB/decade. The third-order filters result in a deeper notch at the tuning frequency than the second-order filter resulting in a greater attenuation of harmonics.

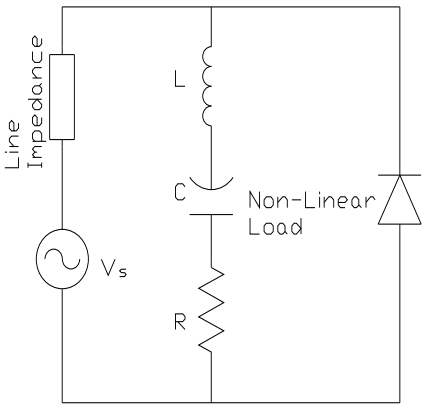

Figure 3.2: Single Tuned Filter

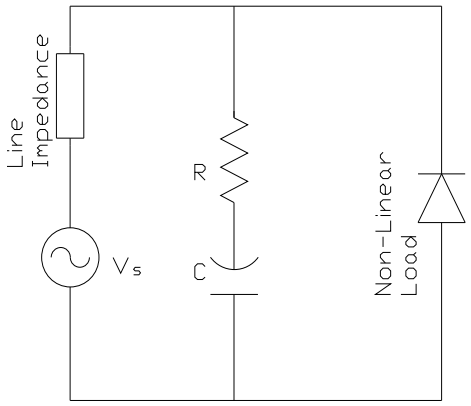

Figure 3.3: First Order Filter

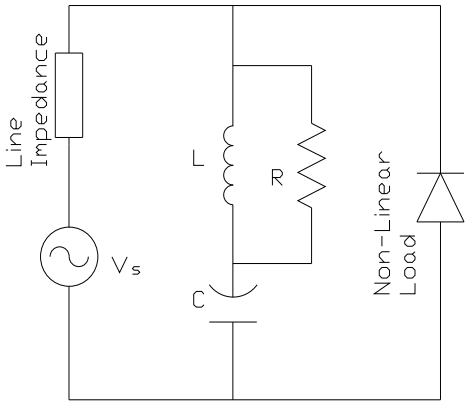

Figure 3.4: Second Order Filter

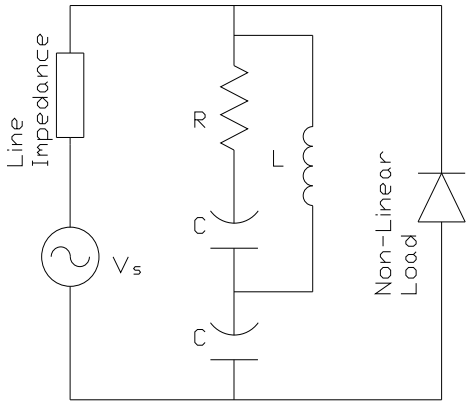

Figure 3.5: Third Order Filter

With the increasing integration of more diverse harmonic loads, continuous tuning of the passive filter becomes increasingly time-consuming and complicated work [51]. Even though passive filters are low-cost and easy to install, the filter's passive elements need to be updated to reflect certain changes in the grid and age

degradation. Passive filter alterations and weaknesses need to be considered for the following:

1) Expansion to the existing distribution system or addition of a new harmonic load in a parallel branch.
2) Any alterations affecting the grid impedance or component aging that affects the lowest impedance path designed for harmonic frequencies.
3) Fast rate of change in the harmonic signature leading to poor transient response [51].
4) Unintentionally creation of resonance conditions due to new localized RLC components added to the grid.
5) Injection of compensating power due to the use of capacitor, as mentioned earlier in the section [52].
6) Non self-tuning functionalities to adapt them with complex dynamic harmonic situation [53].

As an alternative to passive filters, the APF has the capability to change its output current to meet the dynamic nature of non-linear loads and address the disadvantages of the passive filters discussed in this section. The APFs' ability to track certain desired frequency components makes them ideal for harmonic filtering applications.

3.2 Active Power Filters

The basic APF is usually modeled as a controllable current source that uses solid-state switches to inject unwanted harmonic currents with the same amplitude and opposite phase as the non-fundamental currents to maintain a sinusoidal current at source terminals. It provides a considerable upgrade to the problems of the passive filter discussed in the previous section. Since 1970s, APFs have been developed to

enhance the performance of harmonics filtering in the distribution system [54, 55].

They have several advantages in size, multi-harmonic compensation capability, real-time operating capability, and reduced risk of causing harmonic resonance in the power system. The advances in semiconductor technology during the past two decades have stimulated the development and utilization of APF for harmonic elimination and suppression in distribution systems. One of the major factors in the advancement of APF technology is due to the availability of fast self-commutating solid-state devices needed to generate the filter's necessary distribution level output. Hall-effect sensors and better isolation amplifiers have also significantly contributed to enhancing the APF's HD mechanism.

The APF topology can be grouped into four main categories:

1) Shunt Active Power Filters

2) Series Active Power Filters

3) Combined Series Shunt Active Power Filters

4) Hybrid Filters

Each of these APF topologies requires an HD module to estimate the fundamental reference waveform, along with the associated harmonic content to be suppressed. The various APF technologies and operations are described in the following sections.

3.2.1 Shunt Active Power Filters

As the name suggests, Shunt APFs (SAPF) are applied in parallel to the load, and Figure 3.6 shows the basic structure of a stand-alone SAPF. The undesired harmonic current from the non-linear load is represented by I_{har} and combines with the fundamental load current to form the distorted line current, I_d. The distorted line current is processed by the HD algorithm block first to estimate the fundamental

AC component and then generate the residual harmonic reference signal used by the APF converter controller circuit. The power converter is simply used to translate the harmonic waveform to an appropriate magnitude, where it is injected back into the grid with a 180° phase shift.

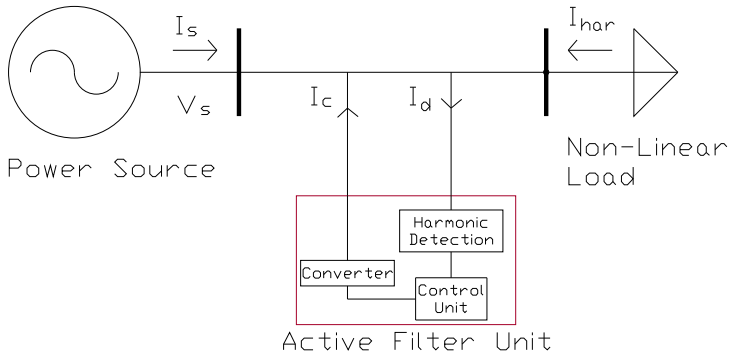

Figure 3.6: Shunt Active Power Filter

The anti-phase harmonic waveform should be generated in a fast, accurate, and timely manner so as not to introduce extraneous distortion in the desired line current. Various HD algorithms used in this research are described in section 3.3, and can be applied to the other APF topologies if desired. The SAPF configuration is the most widely used APF due to its high efficiency [56], potential applicability to expand into other power quality areas, such as voltage flickering and regulations, and for reactive power compensation.

3.2.2 Series Active Power Filters

The series APF is placed in series between the distorting load and the main feeder, as shown in Figure 3.7. Instead of supplying anti-phase harmonic current as the SAPF, the series APF isolates the current flow from one side of the network to another [57]. The filter provides a high-impedance path to the selected harmonics to block the harmonic current flow into the network while providing minimum impedance to the fundamental current.

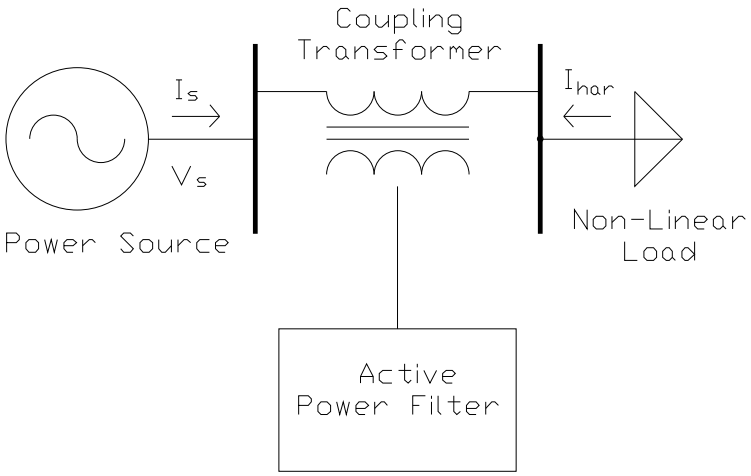

Figure 3.7: Series Active Power Filter

Electric utilities may use this filter type to eliminate the supply voltage flickering or balance the unbalanced load conditions. However, such filters are less attractive as they have to carry high load currents introducing high I^2R loss. It may also produce high converter current levels during the fault condition, which may adversely affect the components in the converter controller circuit [58].

3.2.3 Combined Series Shunt Active Power Filters

This filter combination is also referred to as Universal Active Filter [59-61]. They can effectively compensate harmonics as well as manage voltage flickering, reactive power compensation, and system unbalance problems. The series active filter manages voltage flickering, balances the system voltage, and isolates the voltage harmonics, while the shunt configuration is designed to compensate for the network's harmonic currents and reactive power. The primary disadvantage of this algorithm is the complexity due to the necessity of many switching devices, making the system cost prohibitive [62]. The complex APF architecture is shown in the following Figure 3.8

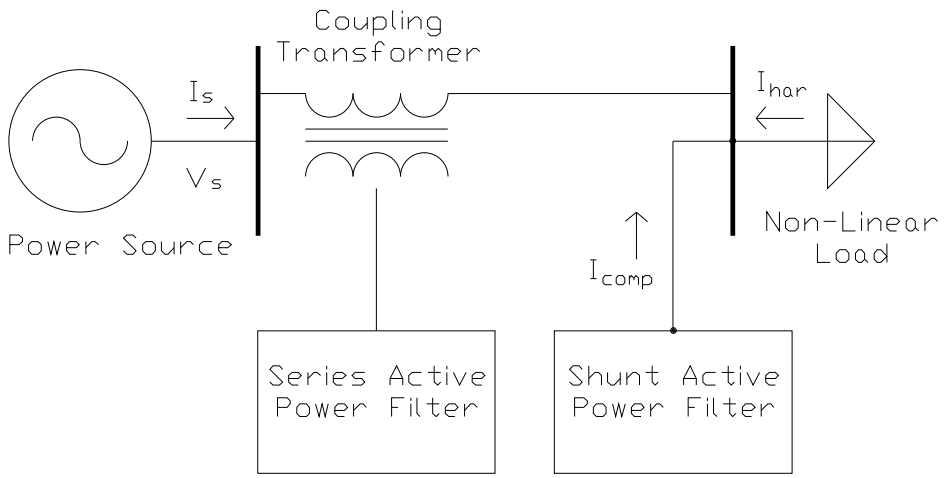

Figure 3.8: Combined Series Shunt Active Power Filter

3.2.4 Hybrid Filters

The hybrid filter combines an APF with one or more passive filters working as a notch filter for selected harmonics compensation or an HPF for total harmonic compensation. A typical combination of SAPF and shunt passive power filter is shown in Figure 3.11. The active segment is designed to compensate for the lower-order dominant harmonics, and the passive counterpart is designed to restrict the higher harmonics [54, 59]. Due to the segmented harmonic compensation of this scheme, the APF has a lower switching frequency, which leads to a low watt-per-pound rating. Even then, the passive filter portion is only suitable for predefined harmonic producing loads since it does not have the self-tuning capability [62]. Hence, the inherent filtering problems associated with passive filters also exist in the hybrid filter implementation.

The hybrid configuration in Figure 3.10 has better filtering capabilities than the basic implementation of the series APF. The active unit aids the passive filter by exhibiting a high impedance for higher-order harmonic frequencies, but there is still a high I^2R loss making the physical implementation of the device inefficient [62]. Figure 3.9 shows a high pass filter that passes all the higher harmonics other than the

fundamental frequency component, and the APF eliminates all the non-fundamental elements. This topology can reduce the dc voltage rating of the switching devices in the controller circuit. However, the tuning limitations of the passive filter portion remain.

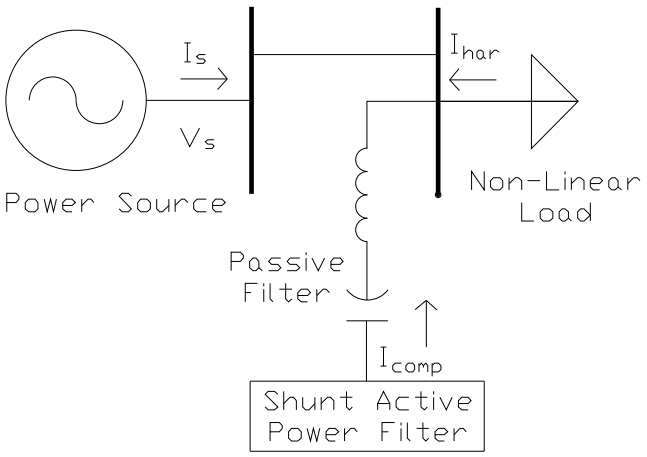

Figure 3.9: Shunt Active in Series Passive

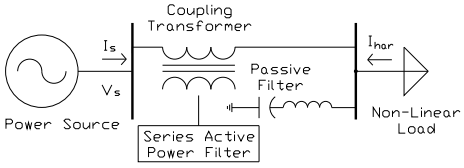

Figure 3.10: Shunt Passive Series Activer

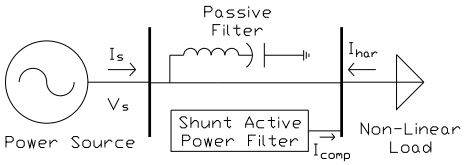

Figure 3.11: Shunt Passive Shunt Active

To assess various HD methodologies, this dissertation will utilize the simple and popular SAPF topology of Figure 3.6 since it has the benefit of shunt configuration without the added complexity of the hybrid implementation.

3.3 APF Harmonic Detection Methods

From the earlier descriptions, the strengths of the APF are clearly discussed. The distinguishing feature between passive and active filtering is the APF's HD capability under difficult harmonic and frequency variation conditions. There exist several HD methods to estimate the fundamental frequency component and residual harmonics, as shown in Figure 3.12. The residual harmonic waveform provides the reference signal for the compensating current generated by the APF. Fast and accurate HD is the key to an effective reduction of the existing line harmonics at specified points in the distribution grid.

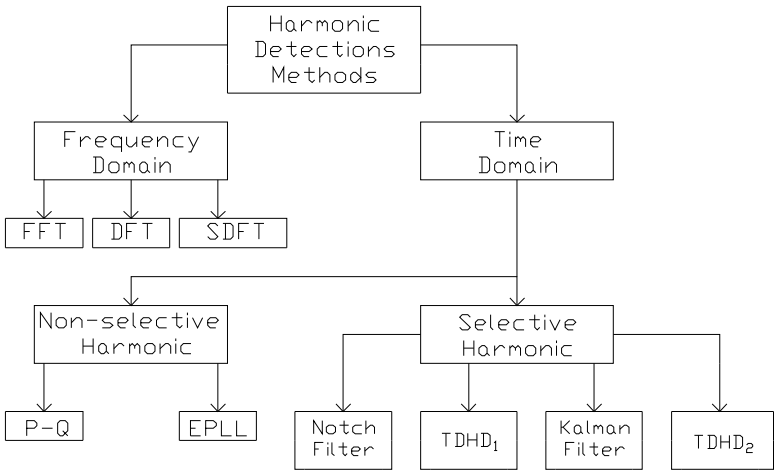

Figure 3.12: Harmonic Detection Methods

In section 1.2, various methodologies for HD have been explored. Figure 3.12 shows that TD methods are subdivided into selective and non-selective groups. The non-selective harmonic approach detects the fundamental frequency component, along with the rest of the combined harmonic signals. It lacks the ability to mitigate specific harmonic orders, which limits the applicability of this type of APF [63]. As an example, known harmonic spectra are usually targeted on the industrial side of the distribution network. This research will focus on the selective HD approach given the flexibility to suppress specific harmonic content. This also makes for a fairer comparison to the FD approach which inherently separates harmonic components.

Two TDHD methodologies under the selective harmonic elimination categories are implemented for this research. One of the renowned TDHD principles is based on the instantaneous reactive-power (P-Q) theory which uses the Park's transformation to convert the distorted AC quantities to DC quantities for harmonic analysis. This technique has some functional limitations as the estimated harmonic waveform contains all the harmonic components. Therefore, this HD principle cannot isolate certain harmonic frequencies, which restricts the flexibility of the algorithm. The $TDHD_1$ method utilizes Direct-Quadrature (D-Q) theory which is an improvement to the P-Q theory since the distorted AC quantity can be transformed to obtain

individual targeted harmonic components.

As discussed earlier, the $TDHD_2$ method can significantly improve the settling time response compared to the $TDHD_1$ and any FDHD methods under certain harmonic situations. The variable step size LMS predictive algorithm is better suited for abrupt changes towards a steady-state convergence without causing a major current surge. The results in chapter 4 will further validate this capability.

The FDHD method used in this research is based on the SDFT and offers reduced computational complexity compared to DFT [64,65]. SDFT can accomplish this by taking advantage of the circular property of the DFT for periodic signals. Equation 3.18 shows SDFT requires one complex multiplication and two complex additions for each new sample of the distorted input. Standard implementations of the DFT (or Fast Fourier Transform, FFT) require an N-dimensional sample space as input and a minimum of $\frac{N}{2}\log_2 N$ complex operations to compute the FD output.

Due to the extensive research on D-Q theory, the $TDHD_1$ filtering performance is well established in APF applications. Correspondingly, the performance of $TDHD_1$ will be the reference to compare against the other two HD methods. The notch and kalman filter classes shown in Figure 3.12 are avoided since complex calculations are required to verify the stability of the non-linear state space equations.

3.3.1 D-Q Harmonic Detection Theory

This TDHD method uses a transformation from a 3-phase stationary coordinate system to the Direct-Quadrature rotating coordinate system [66]. The conversion uses the generalized Park transformation to convert the selected harmonic component from a 3-phase stationary reference frame to a synchronous reference frame. The transformation is essential as it converts the input signals from stationary to rotating frames. The input signal considered for this approach will be the 3-phase co-planar load current $i_{La}(t)$, $i_{Lb}(t)$ and $i_{Lc}(t)$ separated by 120° from each other. The rotating

nature of the transformation is essential for harmonic elimination as it can target various harmonic orders to eliminate from the system under consideration.

The reconstructed DC signals are passed through a Low Pass Filter (LPF) for unwanted harmonics elimination [66]. Equation 3.3 shows that the targeted harmonic current can be measured using this approach. The TDHD_1 approach is a considerable upgrade from the P-Q theory, which is very sensitive to voltage harmonics. The improved HD procedure is independent of voltage harmonics and can perform both total and separate harmonic detections depending on the filtering requirements.

The technique converts the 3-phase AC load currents (i_{La}, i_{Lb}, i_{Lc}) into direct (D) or active component, quadrature (Q) or reactive component, and an extra zero-sequence component (0). The load currents are transformed to separate the harmonic contents from the current fundamental [67]. The transformation is defined by [68]:

$$\begin{bmatrix} i_d(m,t) \\ i_q(m,t) \\ i_0(m,t) \end{bmatrix} = \sqrt{\frac{2}{3}} \begin{bmatrix} \cos(m\omega t) & \cos\left(m\omega t - \frac{2\pi}{3}\right) & \cos\left(m\omega t + \frac{2\pi}{3}\right) \\ -\sin(m\omega t) & -\sin\left(m\omega t - \frac{2\pi}{3}\right) & -\sin\left(m\omega t + \frac{2\pi}{3}\right) \\ \frac{1}{\sqrt{2}} & \frac{1}{\sqrt{2}} & \frac{1}{\sqrt{2}} \end{bmatrix} \begin{bmatrix} i_{La}(t) \\ i_{Lb}(t) \\ i_{Lc}(t) \end{bmatrix} \tag{3.1}$$

Where m is the harmonic order and θ is the angular position of the synchronous reference frame defined by the linear function $m\omega t$, and this reference frame is turning in a constant synchronous speed with the 3-phase voltage [67]. Furthermore, the currents in this reference frame are decomposed into two terms as in Equation 3.2:

$$\begin{bmatrix} i_d(m,t) \\ i_q(m,t) \end{bmatrix} = \begin{bmatrix} \tilde{i_d}(m,t) + \overline{i_d}(m,t) \\ \tilde{i_q}(m,t) + \overline{i_q}(m,t) \end{bmatrix} \tag{3.2}$$

A DC and AC quantity forms the D and Q elements. The harmonic reference current can be extracted from the load currents using a simple LPF with a feed-forward effect. The DC term $\overline{i_d}(m,t)$ and $\overline{i_q}(m,t)$ represent the magnitude of the selected m^{th} order harmonic component and the AC term are rest of the harmonic

components. Equation 3.3 represents the back conversion which is used to convert the extracted DC quantities to the corresponding 3-phase harmonic components of load current

$$\begin{bmatrix} i_a^*(m,t) \\ i_b^*(m,t) \\ i_c^*(m,t) \end{bmatrix} = \sqrt{\frac{2}{3}} \begin{bmatrix} \cos(m\omega t) & -\sin(m\omega t) & \frac{1}{\sqrt{2}} \\ -\cos\left(m\omega t - \frac{2\pi}{3}\right) & -\sin\left(m\omega t - \frac{2\pi}{3}\right) & \frac{1}{\sqrt{2}} \\ \cos\left(m\omega t + \frac{2\pi}{3}\right) & -\sin\left(m\omega t + \frac{2\pi}{3}\right) & \frac{1}{\sqrt{2}} \end{bmatrix} \begin{bmatrix} \overline{i_d}(m,t) \\ \overline{i_q}(m,t) \\ i_0(m,t) \end{bmatrix} \tag{3.3}$$

The 3-phase current $i_a^*(m,t), i_b^*(m,t), i_c^*(m,t)$ are the m$^{\text{th}}$ order harmonic content of the load current

3.3.1.1 TDHD$_1$: D-Q Harmonic Detection

Section 3.3.1 identifies the importance of synchronous rotating frames to capture and mitigate the 3-phase current of various harmonic orders. Convergence of the filters can be significantly increased if selective HD is implemented rather than total harmonic elimination. However, such analysis can only be possible if the harmonic orders present in the distorted signal are known from a prior harmonic evaluation. The dominant harmonic orders need to be calculated through harmonic analysis to determine the synchronous speed of the rotating frames. Also, the inverse transformation matrix is essential for harmonic elimination.

Figure 3.13 shows the basic implementation of TDHD$_1$ where Equation 3.1 is performed in the leftmost block where the 3-phase distorted current signal is the input. The oscillator's output signal controls the reference frame's synchronous speed, and the separation of the DC from the AC occurs in the LPF block. The inverse transformation (Equation 3.3) for the m^{th} order harmonic current takes place in the rightmost block, and its output is the harmonic reference waveform used to control the power converter of the APF for generating the desired compensating current.

The oscillator used to control the synchronous timing is usually PLL, which is

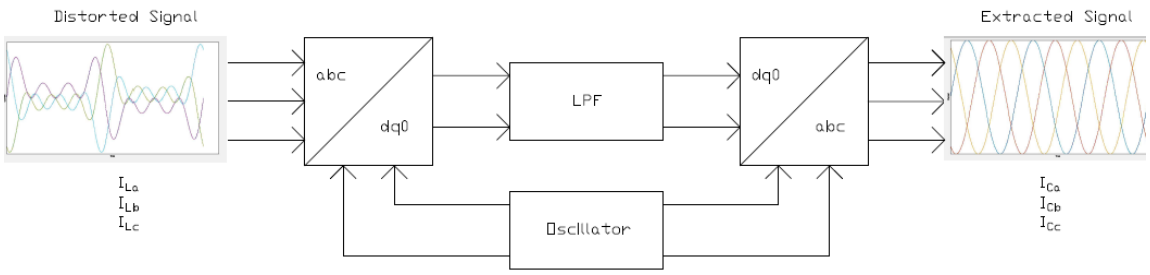

Figure 3.13: $TDHD_1$: D-Q Harmonic Detection Procedure

tolerant to voltage distortion. The output of the oscillator is the exact magnitude required by the final transformation matrix to synchronize with the desired harmonic order present in the input. The adjustable frequency of the oscillator makes the algorithm eligible to perform distinct harmonic order elimination, which was not available for earlier P-Q approaches. From the literature review done for this thesis work, it is evident that $TDHD_1$ harmonic extraction results in reliable HD performance, which will be verified in the simulation results of chapter 4. Figure 3.14 illustrates a certain version of $TDHD_1$ with the selective HD mitigation capability.

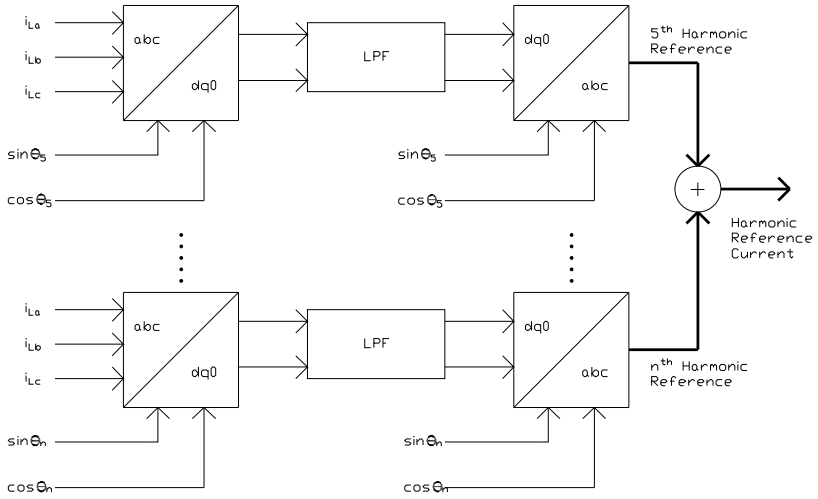

Figure 3.14: Individual D-Q Harmonic Compensation Procedure A

The feeder currents(i_{La}, i_{Lb}, i_{Lc}) are measured and sent through the abc to $dq0$ transformation block for illustrating a 5^{th} order harmonic extraction$(300\,\text{Hz})$, $\sin\theta_5$

and $\cos\theta_5$ are the corresponding synchronous values used in the transformation matrix for the specific harmonic extraction. Once the current transmits through the *abc* to *dq*0 transformation block, the desired harmonic frequency becomes DC, while the undesired harmonic frequencies become AC. In this case for the above blocks of Figure 3.14 the 5^{th} order harmonic current becomes a DC component of the D-Q rotating frame while the other unwanted harmonics result in AC components at different harmonic frequencies.

The LPF eliminates the unwanted AC component leaving only DC signals as input to the *dq*0 to *abc* transformation matrix. The output of this final transformation represents the desired 5^{th} order harmonic reference waveform. The method is repeated for all other desired harmonic components through the block diagram shown in Figure 3.14. The output harmonic reference signal is phase shifted by 180°, then converted to the required line level through the APF converter and injected in the PCC.

Figure 3.15 illustrates an alternative to this HD technique. As seen in this figure, only the fundamental components (i_{a1}, i_{b1}, i_{c1}) are extracted from the input load current (i_{La}, i_{Lb}, i_{Lc}). The compensating current is generated by subtracting the fundamental current from the input current. The final compensation current(i_{Ca}, i_{Cb}, i_{Cc}) is phase shifted 180°, passed through the converter to reach the required line magnitude, and injected in the PCC for total harmonic elimination. Harmonic currents are mitigated by only extracting the fundamental current in this configuration.

In an ideal setup, both version A and B compensation schemes can provide satisfactory performance. The total harmonic compensation (version B) has a faster convergence than the selective harmonic approach as only the fundamental component (60 Hz) needs to be removed from the load current. Harmonics are present in the grid for a shorter time resulting in a dynamic compensating performance. The total harmonic compensation is better suited for non-linear loads with a broader

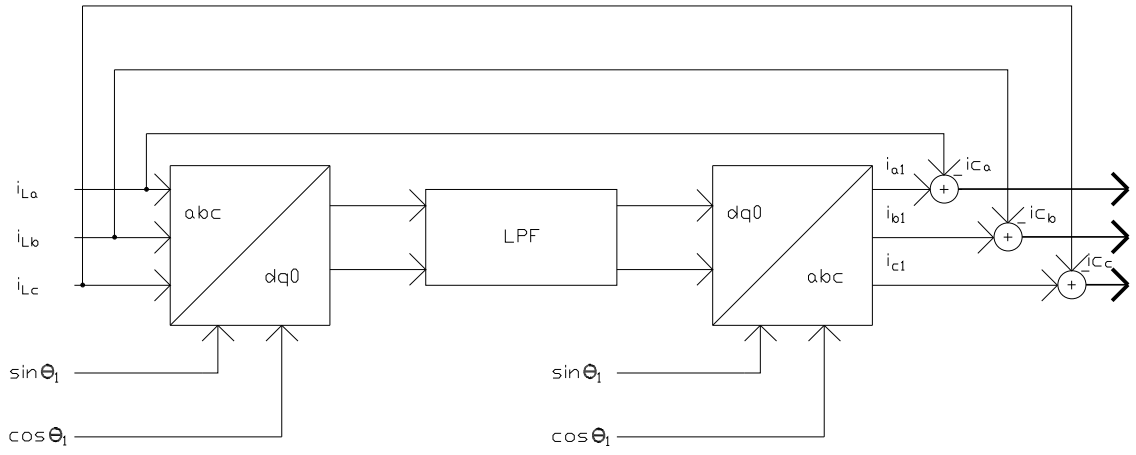

Figure 3.15: Total DQ Harmonic Compensation Procedure B

harmonic spectrum with no specified harmonic operating conditions. The simplistic approach to generate an acceptable current compensation, the phase delay should be fairly marginal. It is in a pole position for implementation in the low-voltage distribution network. In this case, selective HD (version A) is more applicable in known harmonic spectrums with specified operating conditions and is suitable for the industrial setup where balanced network conditions are of priority [69].

3.3.2 $TDHD_2$: Time Domain LMS Adaptive Filtering

Authors from [70-72] introduce the Least Mean Square (LMS) algorithm in detecting the harmonics for the APF applications. The adaptive harmonic canceling algorithm, based on the Wiener method, has been widely used in many signaling applications. It has the capability of self-tuning its parameters [73], a capability that is essential due to the planned extension of the distribution systems and the integration of the extensive non-linear devices with DERs into the grid. The self tuning of the filtering parameters would not have been possible in passive filtering application. The voltage and current level fluctuations due to the weather dependability of the DERs are prominent on the low voltage distribution side. The distorted

current waveform can further deteriorate the system voltage in the vicinity of the DERs [74]. Even the connected loads can be sensitive to the fluctuating voltage, which can further lead to the protection system tripping [75].

Fast and accurate estimation of the fundamental waveform is required by an APF using the $TDHD_2$ technique. The adaptive algorithm can approximate the amplitude and phase of the fundamental current(i_{a1}, i_{b1}, i_{c1}) in a fast manner under various dynamic conditions such as unbalanced load removals and alterations in solar radiations intensity. The desired harmonic content can be measured as the difference between the fundamental current and the distorted load current(i_{La}, i_{Lb}, i_{Lc}) [76].

The closed-loop adaptive filtering is better suited for its self-tuning abilities in 3-phase power system. The traditional LMS algorithm has some level of error in the initial stage and a slow settling time for steady-state convergence. Alternately, this research will investigate variable step-size predictive control-based LMS algorithms for harmonic detection. This work provides the necessary improvements to solve the associated problems of the conventional approach. Compared to the fixed step-size LMS algorithm, the implemented algorithm has a good convergence properties, reduced steady-state error, and noise immunity [27]. Further details are provided in subsubsection 3.3.2.2.

3.3.2.1 Traditional Predictive Control

The principle behind the predictive control uses the present data and previous M input to predict the system's output. Figure 3.16 shows the block diagram of the predictive control algorithm, and the conventional LMS algorithm is used to optimize the parameters of the predictive model [28]. $X\,(n)$ is the previous M sequence input data to the predictive model written as:

$$X\,(n) = \begin{bmatrix} x\,(n) & x\,(n-1) & x\,(n-2) & \ldots & x\,(n-M+1) \end{bmatrix} \tag{3.4}$$

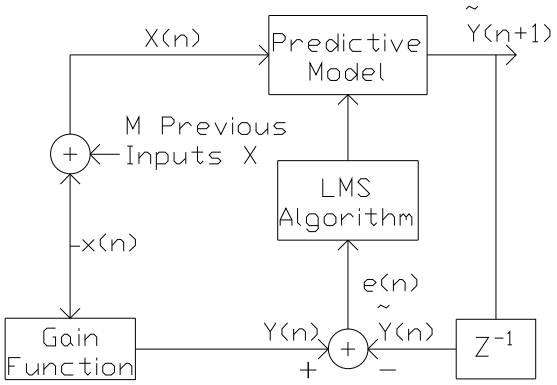

Figure 3.16: Predictive Control Using LMS Algorithm

$$W(n) = \begin{bmatrix} w_0(n) & w_1(n) & w_2(n) & \dots & w_{M-1}(n) \end{bmatrix} \tag{3.5}$$

where $W(n)$ is the weight coefficient vector of the predictive model and $\tilde{Y}(n+1)$ is the output of the predictive model presented as:

$$\begin{aligned} \tilde{Y}(n+1) &= w_0(n)\,x(n) + w_1(n)\,x(n-1) + \dots + w_{M-1}(n-M+1)\,x(n-1) \\ &= \sum_{j=0}^{M-1} w_j(n)\,x(n-j) \\ &= W(n)\,X^T(n) \end{aligned} \tag{3.6}$$

Comparing the predictive outcome with the actual outcome gives the error output of the filter as below:

$$\begin{aligned} e(n) &= Y(n) - \tilde{Y}(n) \\ &= Y(n) - W(n)\,X^T(n) \end{aligned} \tag{3.7}$$

Implementing the LMS algorithm, the optimal $W(n)$ to minimize the $E\{e^2(n)\}$ is

recorded by performing the following operations

$$\frac{\partial\Big[E\{e^2(n)\}\Big]}{\partial\Big[W(n-1)\Big]} = 2E\Big\{X^T(n-1)\Big[W(n-1)X^T(n-1)\Big] - Y(n)X^T(n-1)\Big\}$$
$$= 2E\Big\{X^T(n-1)e(n)\Big\} \tag{3.8}$$

For further simplification, $X^T(n-1)$ is replaced with $X(n-1)$ and the iterative formula for the filter weight updates is:

$$W(n) = W(n-1) + 2\mu E\Big\{X(n-1)e(n)\Big\} \tag{3.9}$$

The performance is not ideal when using the traditional fixed step size algorithm to measure the harmonic components. The primary reason is the settling time and steady-state accuracy. A larger step size results in a faster convergence but results in a larger error. On the other hand, a small step size results in a small, steady-state error, but the convergence of the filtering action is slow. A conventional LMS with a fixed μ is generally considered unsuitable for simultaneously achieving a good settling time and minimum steady-state error

3.3.2.2 Predictive Control with Variable Step

An updated algorithm using variable steps of μ is designed to compensate for the drawbacks of the conventional LMS algorithm for the harmonic compensation [27]. The new algorithm implements the past error data and updates the predictive model by power weights of error which vary with a forgetting factor. The iterative operation

of the $W(n)$ and $\mu(n)$ are updated with the equations from [77].

$$
\begin{aligned}
W(n) &= W(n-1) + 2\mu(n) E\Big\{ X(n-1) e(n) \Big\} + k\Big[W(n-1) - W(n-2) \Big] \\
\mu(n) &= \alpha\mu(n-1) + \eta\beta(n) \rho^2(n) \\
\rho^2(n) &= \sum_{j=0}^{M-1} \lambda(j) e^2(n-j) \\
\lambda(j) &= e^{-\frac{j}{2}} \\
\beta(n) &= \Big| \zeta(n) \Big|^h \\
\zeta(n) &= \gamma\zeta(n-1) + (1-\gamma) e(n)
\end{aligned}
\tag{3.10}
$$

where α, k, γ, h and β are constants limited by:

$$
\begin{aligned}
&0 < \alpha, k, \gamma, \beta < 1 \\
&1 < h < 2
\end{aligned}
\tag{3.11}
$$

The constants are referred from [78], where $\beta(n)$ is the follow up factor, $\lambda(j)$ represents the forgetting factor and $\rho^2(n)$ is the power weights of the error. From Equation 3.10, $\mu(n)$ is dependent on two variables, the first is the power weights of the error $\rho^2(n)$ and the second one is the follow-up factor $\beta(n)$ affected by $e(n)$. $\rho^2(n)$ reflects the importance of previous error data and exponential function $\lambda(j)$ can reduce the impact of noise interference. $\beta(n)$ is dependent on the average estimation of error $\zeta(n)$. Increases in $\beta(n)$ forces the $e(n)$ to follow and this characteristic enhances the inter-dependence between μ and $e(n)$. The constant h is used to regulate the sensitivity of $\beta(n)$ to $\zeta(n)$.

In the initial stage of the filter operation, $\mu(n)$ is set at $\frac{2}{\bar{\lambda}_{max}}$ to speed up the convergence. During the convergence process, error and $\mu(n)$ decrease simultaneously

until it reaches stability. For system stability, the following constraint is imposed

$$\mu = \begin{cases} \frac{2}{\overline{\lambda}_{max}} & \mu > \frac{2}{\overline{\lambda}_{max}} \\ \mu & 0 < \mu < \frac{2}{\overline{\lambda}_{max}} \\ 0 & \mu < 0 \end{cases} \tag{3.12}$$

where $\overline{\lambda}_{max}$ is the eigenvalue of the autocorrelation matrix of the input signal $X(n)$. Finally, the block diagram for the single-phase action is shown in the Figure 3.17. α=0.97, β=3 $\times$ 10^{-5}, γ=7.65 $\times$ 10^{-4} , h=1.77, and k=0.95 is determined from SIMULINK simulations. Repeated simulations were done and the constants were updated till a minimum steady state error is achieved which is comparable to the TDHD_1 results.

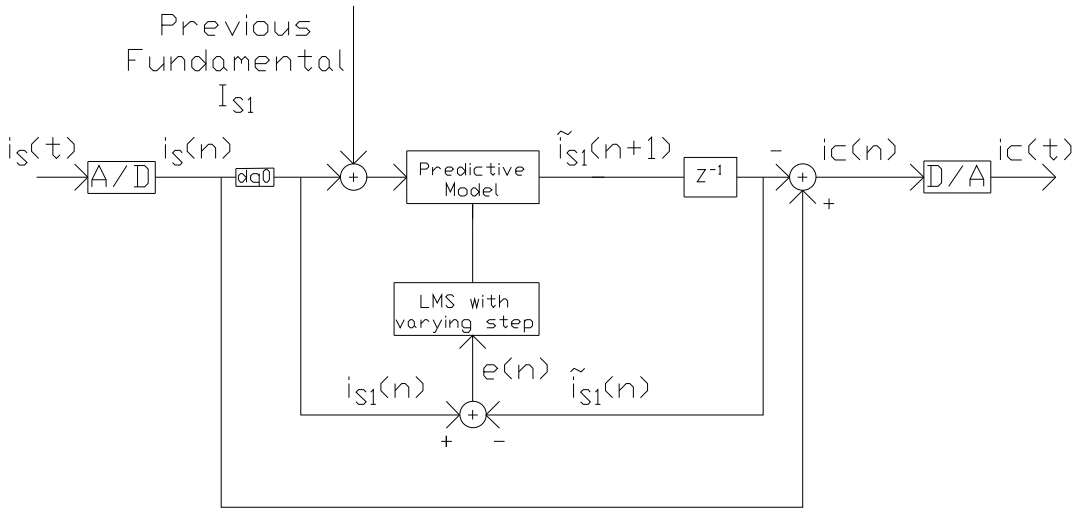

Figure 3.17: Harmonic Detection Using Predictive Control

Here the $i_S\,(n)$ denotes the sampled current connected to the load side feeders. $i_{S1}\,(n)$ is the fundamental component extracted by the D-Q transformation mentioned in subsection 3.3.1. Replacing $X\,(n)$ with $i_{S1}\,(n)$ the filter weights can be represented as

$$W(n) = W(n-1) + 2\mu(n) E\Big\{ i_{S1}(n-1)\, e(n) \Big\} + k\Big[W(n-1) - W(n-2) \Big] \tag{3.13}$$

The component of the fundamental frequency (60 Hz) is easier to predict, and the predictive control of TDHD_2 outputs the forecast of fundamental current $\tilde{i}_{S1}(n)$ which can be represented as

$$\tilde{i}_{S1}(n+1) = W(n)\, i_{S1}(n)^{\mathrm{T}} \tag{3.14}$$

The input to the harmonic detection block is the previous input of the fundamental current extracted from the load side. Finally, subtracting the $\tilde{i}_{S1}(n)$ from $i_S(n)$, we get the compensation current $i_c(n)$ to feed the converters for producing the required compensating current. Chapter 4 will further analyze the validation of the results.

3.3.3 SDFT: Sliding Domain Fourier Transform for HD

Frequency analysis can be advantageous over performing the same analysis in the TD. The advantage is its clear presentation of the fundamental and harmonic components present in a signal. A significant barrier to FD processing is the required computation load involved in the FT [79]. The generalization of the FT in discrete time signals is implemented using the DFT. This generalization, however, assumes certain characteristics of the discrete time signal in terms of periodicity and sampling rate, and requires a finite sample set as an input. This can represent a significant computational burden, even for the highly efficient methods of the DFT (i.e. Fast Fourier Transform (FFT)). The author in [80] points out the time delay as the FFT's most significant drawback since a minimum of one entire fundamental cycle is required to compute the spectral decomposition of the signal. Further analysis of

this methodology is provided in the following subsections.

3.3.3.1 SDFT Principle

If a discrete-time signal is given as follows

$$..., x(-2), x(-1), x(0), x(1), x(2), ..., x(n), x(n+1) \tag{3.15}$$

At the time instant n, a windowed sequence $x(n)$ consisting of N samples, is formed as

$$x(n) = \{x(n-N+1), x(n-N+2), ..., x(n-1), x(n)\} \tag{3.16}$$

The corresponding DFT operation with a sample size of N results in

$$X(n) = \{X_0, X_1, ..., X_{N-2}, X_{N-1}\} \tag{3.17}$$

From the equations above, it can be seen for a new value of n; a new DFT sequence needs to be computed. For the harmonic filtering application, every time there is a new input, an entire period is needed to be computed to determine the existing spectra in the system [81]. In other words, the FFT algorithm requires a new sequence of the sampled waveform for every new value of n. However, in the scenario when the harmonic algorithm demands only the k^{th} term of the DFT (X_{k-1}), the FFT is clearly inefficient.

The SDFT avoids this repeating demand of filling the sampling fixed-length buffer as it can give the k^{th} term of the DFT without needing the Fourier transform of the entire previous dataset. In other words, the sampling window moves or slides along the TD stream one sample at a time [82]. SDFT principle is based on the DFT shifting theorem commonly known as the circular shift property [83]. It states that

if

$$x\left(n\right) \xrightarrow{N-DFT} X_k\left(n\right)$$

where X_k is the spectral component, and k is the DFT bin of interest, then the circular DFT shift of the sequence becomes

$$x\Big[\left(n-m\right)_N\Big] \xrightarrow{N-DFT} X_k e^{-j\frac{2\pi}{N}km}$$

Then DFT of the sequence circularly shifted by one sample is :

$$x\Big[\left(n+1\right)_N\Big] \xrightarrow{N-DFT} X_k e^{j\frac{2\pi}{N}k}$$

The spectral components of the shifted time sequence are the original spectral components multiplied by $e^{j\frac{2\pi}{N}k}$. Authors from [84] derived the final expression as:

$$X_k\left(n\right) = X_k\left(n-1\right)e^{j\frac{2\pi}{N}k} - x\left(n-N\right) + x\left(n\right) \tag{3.18}$$

where $X_K\left(n\right)$ is the new spectral component and $X_K\left(n-1\right)$ is the previous spectral component. Figure 3.19 shows the shifting window implemented on the signal to compute the required transform. From Equation 3.18, it can be seen to get to the new spectrum, the previous spectral component needs to have a phase shift operation. In contrast to the phase shift operation, there needs to be an addition of $x\left(n\right)$ and a subtraction of $x\left(n-N\right)$. The computational complexity for the SDFT is $O\left(N\right)$ compared to $O\left(N^2\right)$ of DFT and $O\left(N\log_2\left(N\right)\right)$ of FFT. From the Figure 3.18, it can be seen as the sample size increases, the computational requirements of FFT compared to SDFT increases exponentially. SDFT overcomes this shortfall by processing the input sample by sample.

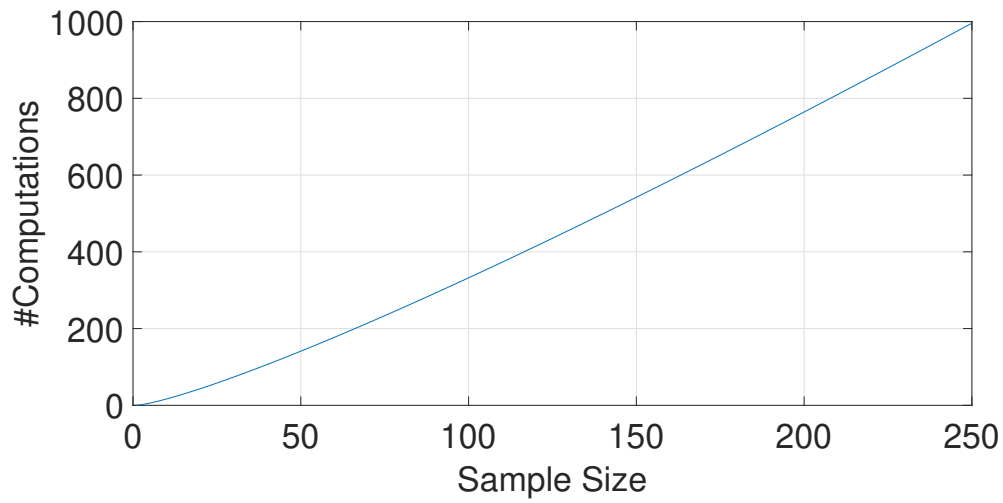

Figure 3.18: #Computations vs. Sample Size

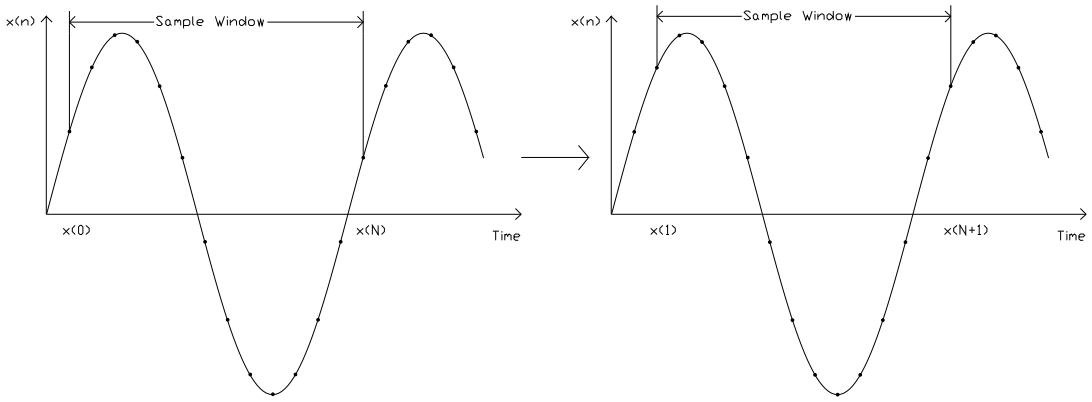

Figure 3.19: SDFT Shifting Principle

The computation steps have been considerably reduced using the SDFT, limiting phase delay in the processing operation [85]. The proposed spectral component detection is shown in Figure 3.20

3.3.3.2 SDFT APF Implementation

The HD methodology based on the SDFT is able to perform a reliable estimation of the reference current without restriction on the electrical power sources

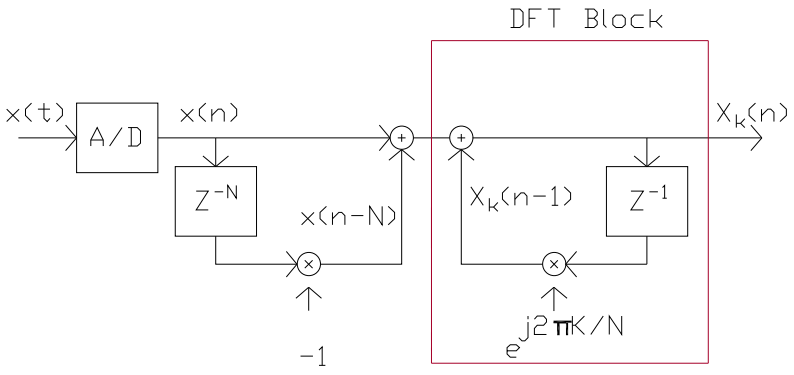

Figure 3.20: Block Diagram of the Spectral Component Detection

and loads [85]. The connected loads can be balanced or unbalanced, and the feeder current can be prone to disturbance. The SDFT algorithm can efficiently extract the fundamental current and perform harmonic suppression. The SDFT algorithm is performed N times per fundamental period, and the sampling period is calculated as:

$$T_s = \frac{T_1}{N} \tag{3.19}$$

where T_1 is the fundamental period, N number of samples per fundamental period, and T_s is the sampling period. The algorithm is performed N times per entire cycle. The compensating current generated by the APF for a balanced three-phase system is:

$$\begin{aligned} ic_a(t) &= is_a(t) - i_{a1}(t) \\ ic_b(t) &= is_b(t) - i_{b1}(t) \\ ic_c(t) &= is_c(t) - i_{c1}(t) \end{aligned} \tag{3.20}$$

The feeder current is passed through an analog-to-digital converter with a sampling time of T_s. The Equation 3.18 is written as follows to calculate the first harmonic

spectral component of the corresponding phases' feeder currents:

$$\begin{aligned} IS_{a1}(nT_s) &= IS_{a1}((n-1)T_s)\,e^{j\frac{2\pi}{N}} - is_a((n-N)T_s) + is_a(nT_s) \\ IS_{b1}(nT_s) &= IS_{b1}((n-1)T_s)\,e^{j\frac{2\pi}{N}} - is_b((n-N)T_s) + is_b(nT_s) \\ IS_{c1}(nT_s) &= IS_{c1}((n-1)T_s)\,e^{j\frac{2\pi}{N}} - is_c((n-N)T_s) + is_c(nT_s) \end{aligned} \tag{3.21}$$

where $is_a(n)$, $is_b(n)$ and $is_c(n)$ are the discrete signal representing the feeder side currents. $IS_{a1}(n)$, $IS_{b1}(n)$ and $IS_{c1}(n)$ are the fundamental spectral component of the corresponding phase currents. $IS_{a1}(n-1)$, $IS_{b1}(n-1)$, $IS_{c1}(n-1)$ are the previous fundamental component of the corresponding phase currents. The value of k is 1 due to the first harmonic reference frame.

For a phase angle of zero between the mains voltage and the extracted fundamental current, the fundamental current equation is

$$\begin{aligned} is_{a1}(nT_s) &= \frac{2}{N}\left|IS_{a1}(nT_s)\right|\sin(2\pi 60(nT_s)+\phi_a) \\ is_{b1}(nT_s) &= \frac{2}{N}\left|IS_{b1}(nT_s)\right|\sin(2\pi 60(nT_s)+\phi_b) \\ is_{c1}(nT_s) &= \frac{2}{N}\left|IS_{c1}(nT_s)\right|\sin(2\pi 60(nT_s)+\phi_c) \end{aligned} \tag{3.22}$$

The resulting compensating current equation by implementing Equation 3.22 and Equation 3.20 is:

$$\begin{aligned} ic_a(nT_s) &= is_a(nT_s) - \frac{2}{N}\left|IS_{a1}(nT_s)\right|\sin(2\pi 60(nT_s)+\phi_a) \\ ic_b(nT_s) &= is_b(nT_s) - \frac{2}{N}\left|IS_{b1}(nT_s)\right|\sin(2\pi 60(nT_s)+\phi_b) \\ ic_c(nT_s) &= is_c(nT_s) - \frac{2}{N}\left|IS_{c1}(nT_s)\right|\sin(2\pi 60(nT_s)+\phi_c) \end{aligned} \tag{3.23}$$

For an imbalanced scenario, authors in [86] referred to the following equation:

$$
\begin{aligned}
ic_a\left(nT_s\right) &= is_a\left(nT_s\right) - \frac{2}{3N}\left(\left|IS_{a1}\left(nT_s\right)\right| + \left|IS_{b1}\left(nT_s\right)\right| + \left|IS_{c1}\left(nT_s\right)\right|\right)\sin\left(2\pi 60\left(nT_s\right) + \phi_a\right) \\
ic_b\left(nT_s\right) &= is_b\left(nT_s\right) - \frac{2}{3N}\left(\left|IS_{a1}\left(nT_s\right)\right| + \left|IS_{b1}\left(nT_s\right)\right| + \left|IS_{c1}\left(nT_s\right)\right|\right)\sin\left(2\pi 60\left(nT_s\right) + \phi_b\right) \\
ic_c\left(nT_s\right) &= is_c\left(nT_s\right) - \frac{2}{3N}\left(\left|IS_{a1}\left(nT_s\right)\right| + \left|IS_{b1}\left(nT_s\right)\right| + \left|IS_{c1}\left(nT_s\right)\right|\right)\sin\left(2\pi 60\left(nT_s\right) + \phi_c\right)
\end{aligned}
\tag{3.24}
$$

Implementing the Equation 3.24, the control circuit for the harmonic compensation current is built as the Figure 3.21.

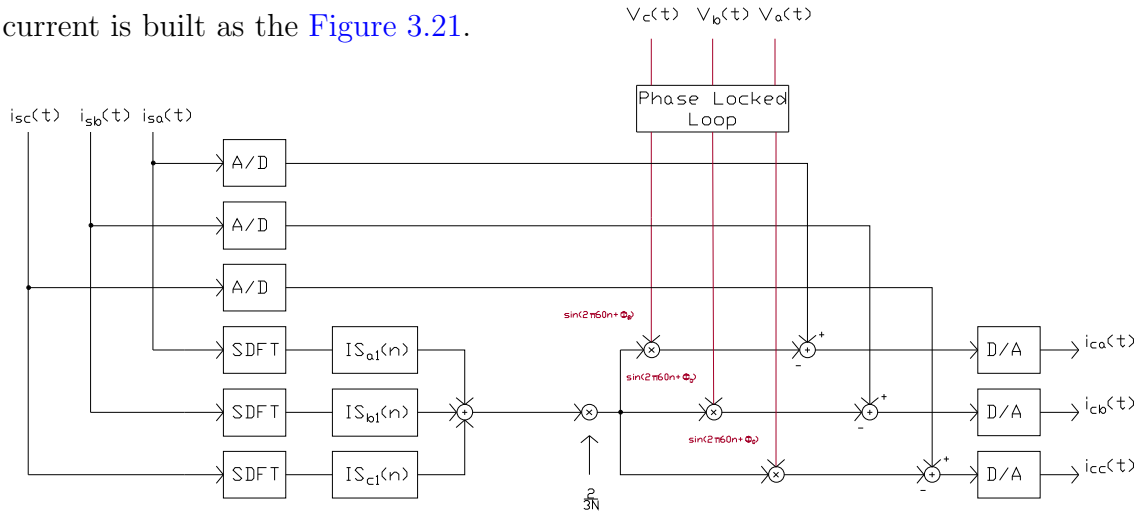

Figure 3.21: Block Diagram for Compensation Current Generation Using SDFT

In the summing block, the resultant magnitude of the spectral components is added and later passed through the multiplier and subtracted with the appropriate signals to generate the required compensating currents. For the SDFT HD, the APF settling time response is comparably faster to earlier FT-based implementations [87-89]. The SDFT algorithm efficiently reduces the operation time for the filtering action in the FD and allows fast and accurate detection of harmonic contents.

Chapter 4

Results and Analysis

This chapter provides the simulation results of the proposed APF HD methods under several different harmonic situations. The simulation for the APF evaluation was done using MATLAB as it has the tools to create realistic power electronic models using the SIMULINK environment. A wide range of parameters dealing with the device-level operation of the APF are available according to the desired configuration. The basic SIMULINK APF workspace is shown in Figure 4.1. The Simscape library is primarily used for implementing the APF and the control systems toolbox is used to determine the settling time. The settling time is defined as the time response to reach and stay within 2% of the final value [90].

The main objectives of the harmonic tests will be to determine the capability of the APF and to reduce the TDD of the source current while the magnitude of current at the load and source are continuously tracked for their harmonic signature. The source current TDD is taken into consideration as most of the protection device coordination is dependent on the parameters of the source current. However, both the load and the source current will be tracked to record the harmonic suppression and measure the effectiveness of the APF HD applied on the simulation environment. For all test cases, harmonic elimination is applied up to the 30^{th} order of fundamental frequency to ensure all the significant harmonic frequencies are reduced and if any frequency deviation occurs is captured in the harmonic analysis window.

The following assumptions are made to simplify the accuracy of the simulations:

1) The average power demand of a Canadian home is 1.23 kW [91]. It is as-

sumed the distribution transformers are connected to 16 residences, which is a reasonable number for a typical Canadian residential electrical network. The non-linear load is having a poor power factor for intentional harmonic injection. The PVs harmonic output for the test simulation is 1 kW and is included in the non-linear load.

2) The source voltage is considered ideal and free of harmonics as the loads modelled are thyristor loads and only affect the current waveform. No distortion will be suffered by the voltage waveform parameters.

3) The PLL is in the APF block to extract the source frequency required for the Park's transformation.

4) The inductance, capacitance and resistance values do not change over time and no internal parasitic reactance is formed during the validation of our simulations.

5) For the simplicity of APF performance, the load current is considered to be the rated current to highlight the effectiveness of the APF algorithm.

The APF HD evaluation will be judged based on four test cases:

- ▷ Test case 1: steady-state analysis;
- ▷ Test case 2: active load fluctuation;
- ▷ Test case 3: reactive load fluctuation;
- ▷ Test case 4: non-linear load replacement.

The test cases were chosen as the distribution system will have load variations based on active and reactive power during the normal course of grid operation. The APF needs to have a robust HD algorithm to accommodate this variation over its operational cycle.

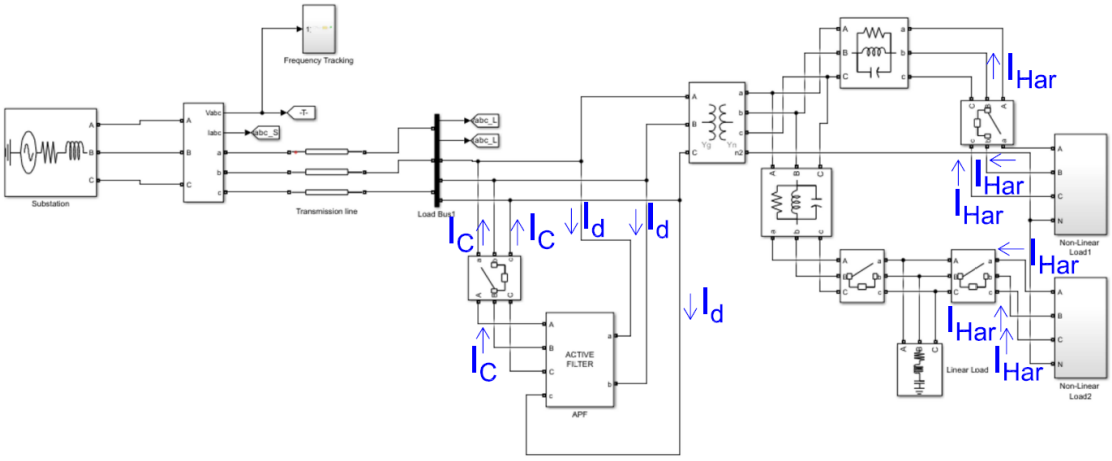

Figure 4.1: Simulink APF Diagram

4.1 Test Case 1: Steady-State Analysis

The objective here is to ensure the convergence properties of the APF HD methods and measure how accurately the harmonic distortion is removed from the distribution system. The resulting current waveform from a combination of 15 kVA non-linear load (13 kW,7.5 kVAR) connected to a 10 kVA (8.5 kW,3.87 kVAR) linear load is shown in Figure 4.2. The percentage of non-linear load is higher than the linear load as rooftop PVs are also included in the test. The ratio between the harmonic load and linear load may not be this extreme in practice but was done to ensure the effect of the APF could be clearly measured. The ratio of non-linear and linear load for this test case also represents the initial conditions for the test cases to follow.

The APF will be switched on after 0.5 s to record the load current and source current TDD levels in the power system.Once the APF is turned on, Figure 4.3 shows the APF outcome on the source side current waveform for the $TDHD_1$ method. $TDHD_1$ performs well to stop the migration of the harmonics into the generation side. Before the APF activation, current waveform at the source side (Figure 4.3 current waveform before 0.5 s) and load side (Figure 4.2) have the same harmonic

signature. After the APF activation, the harmonic content at the source side has been considerably reduced, shown in Figure 4.6. The TDD at the source current decreases from 47.84% to 3.75% with a settling time of 0.01 s.

For $TDHD_2$, the TDD level is measured to be 1.32% which is slightly lower if compared with $TDHD_1$ but has a longer settling time of 0.10 s. As expected, the stable output current of Figure 4.4 closely resembles the output of $TDHD_1$ in Figure 4.3. The TDD measured for the SDFT method is the lowest among the three HD methods investigated in this part of the research part where TDD level falls to 0.47% and the settling time was measured at 0.004 s. The SDFT result shows an impressive capability in harmonic reduction and settling time. This indicates the merit of processing harmonics in the FD.

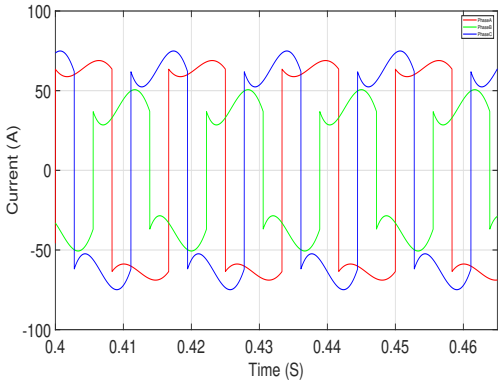

Figure 4.2: Non-Linear Current

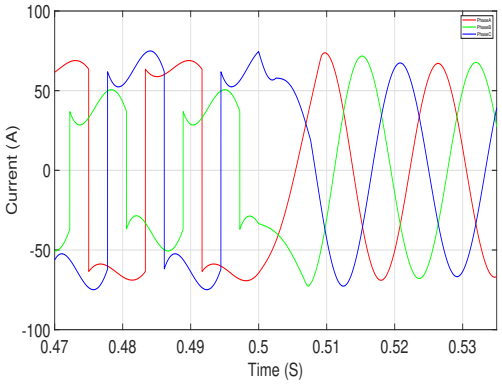

Figure 4.3: $TDHD_1$ Output

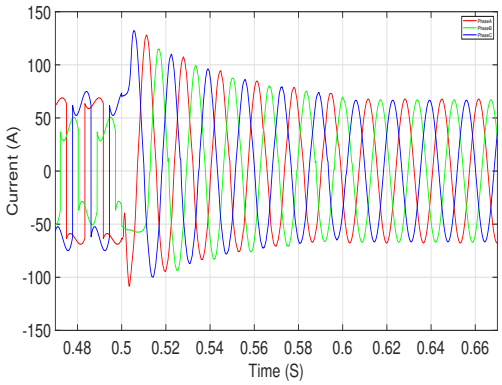

Figure 4.4: $TDHD_2$ Steady-State Output

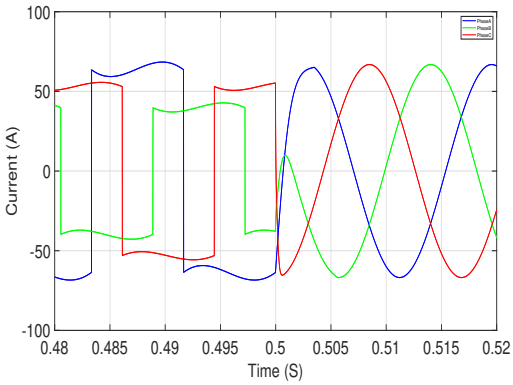

Figure 4.5: SDFT Steady-State Output

In a comparison of the TD based methods, $TDHD_2$ has slower convergence but

has better harmonic mitigation than $TDHD_1$ due to the application of the predictive algorithm used. A reduced setting time duration of $TDHD_2$ could be achieved by using a more aggressive LMS step change of $\mu(n)$ but this would sacrifice its TDD performance. Decisions on which HD method to implement should be based on the desired TDD level and settling time duration. The harmonic levels for all three HD methods are given in Figure 4.6.

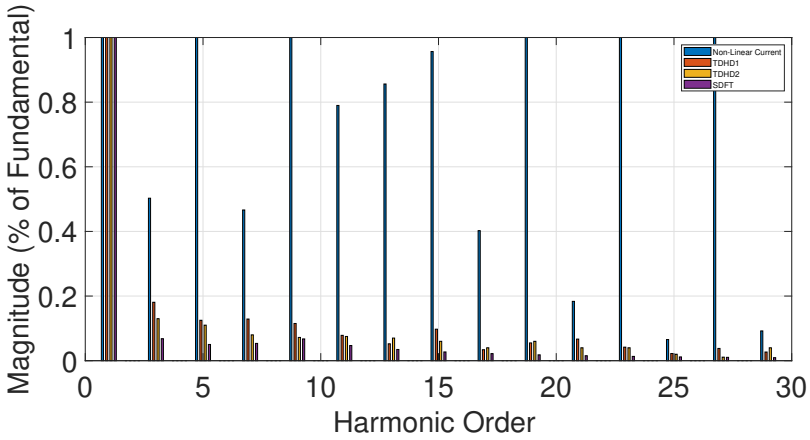

Figure 4.6: Harmonic Content at Steady-State

4.2 Test Case 2: Active Load Fluctuation

In this test case, the active power of the connected linear load will be increased and then decreased after a certain duration. This test case validates the APF current tracking capability after a change in load. For our analysis the linear load is increased to 50 kW at t=1 s and then shredded to 44 kW at t=2 s, and, if the APF fails to converge, the utilized HD method may not be suitable for this operating condition. The HD methods is expected to withstand this change in current magnitude as it will be a frequent phenomenon in any distribution system.

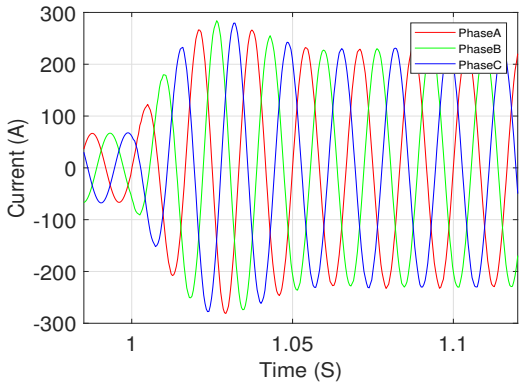

Figure 4.7: $TDHD_1$ Active Load Increase

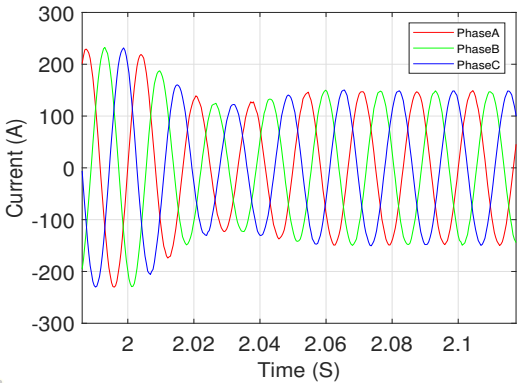

Figure 4.8: $TDHD_1$ Active Load Decrease

After the load addition, the $TDHD_1$ TDD is 0.61% and the line currents converged to stable magnitude within 0.06 s. With load shredding shown in Figure 4.8, the TDD is 1.98%, and the settling time for load shredding is measured to be 0.07 s. For $TDHD_2$, the TDD is measured to be effectively the same at 0.33% and 0.32% for the load increase and shredding respectively. Settling time is a bit longer than the $TDHD_1$ method, no overshoots are observed. For both the load addition and shredding the settling time is 0.10 s. Again, $TDHD_2$ has improvements in harmonic reduction but with poorer settling times.

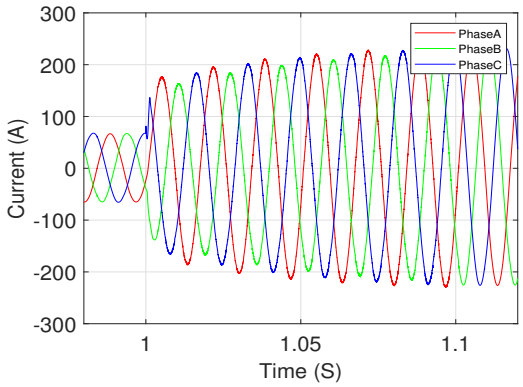

Figure 4.9: $TDHD_2$ Active Load Increase

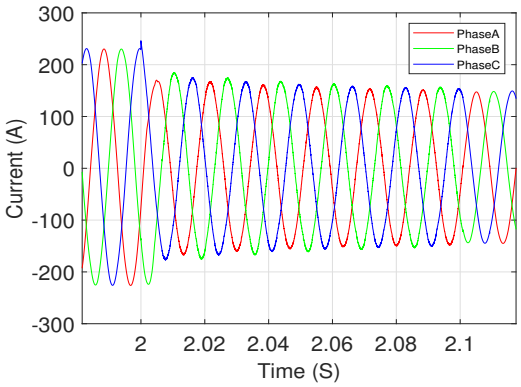

Figure 4.10: $TDHD_2$ Active Load Decrease

For SDFT, the TDD after load increase is measured to be the lowest among the three HD algorithms at 0.11%. After the load decrease, the TDD is measured to be

the lowest value of 0.12%. Steady-state values have been reached within 0.08 s which is comparable to both TD methods. Figure 4.11 and Figure 4.12 illustrate the APF output using SDFT.

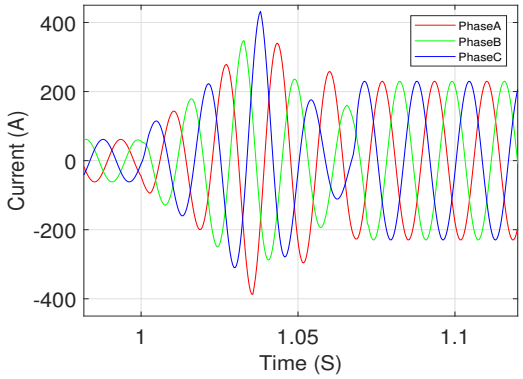

Figure 4.11: SDFT Active Load Increase

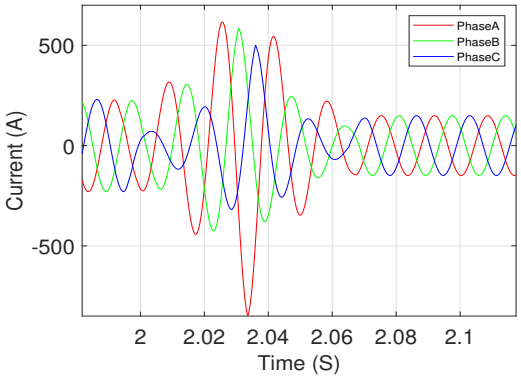

Figure 4.12: SDFT Active Load Decrease

Also, during load shredding and addition, frequency deviations can occur depending on the amount of the dynamic load change. This frequency deviation will lead to an inaccurate estimation of the true line harmonics unless the system frequency is tracked. If the fundamental signal component has a frequency displaced slightly from the filter centre frequency, harmonic energy shifts within the sinc function interpolation inherent to the DFT [92]. In our case, the use of a PLL avoids any frequency deviation issues as the nominal frequency is continuously tracked, preventing any misinterpretation of the line harmonic frequencies.

The various harmonic frequency components for each HD method are shown in Figure 4.13 and Figure 4.14. From the results, $TDHD_2$ and SDFT approach is shown to haver a better harmonic compensation than $TDHD_1$. As the harmonic order increases, the accuracy of the harmonic compensation of the SDFT outperforms the two other HD methods. Settling time of SDFT and $TDHD_1$ are comparable while $TDHD_2$ is highest due to its adaptive LMS filtering implementation.

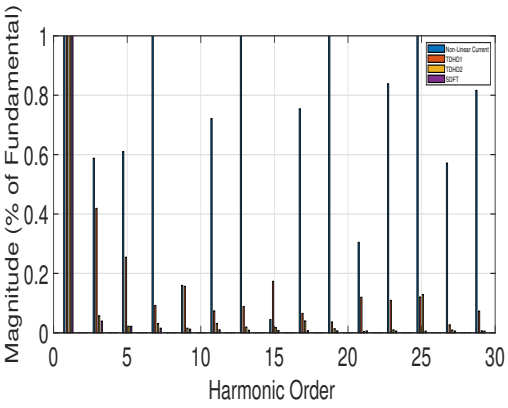

Figure 4.13: Harmonic Content for Active Load Increase

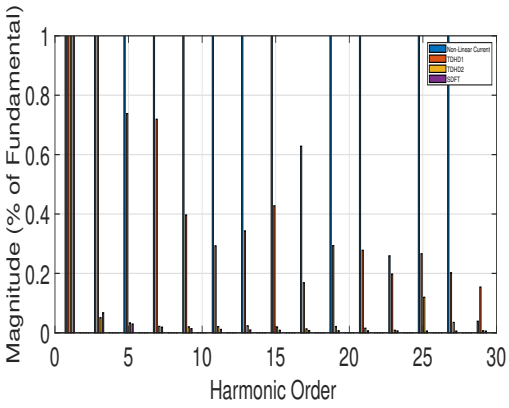

Figure 4.14: Harmonic Content for Active Load Decrease

4.3 Test Case 3: Reactive Load Fluctuation

This test case is designed to investigate the APF HD performance during a sudden variation of reactive power on the grid. An unwanted reactive power injection can come from the transmission line capacitance when the connected load in the distribution system is low, particularly at night [93]. Also, changes in inductive loads from industrial feeders will affect reactive power conditions on the grid. The resulting phase change between the voltage and current from these load changes could impact the APF performance in terms of TDD and settling time performance. To simulate a large industrial load, a lagging load of 40 kVAR is added at t=1 s and reduced to 36 kVAR at t=2 s.

Both settling times for TDHD_1 after t =1 s and t =2 s is measured to be 0.02 s. The TDD level after the increase in reactive power is recorded 1.18% while after load shredding the TDD is measured 1.44%. The current at the source terminals does not have significant distortions which is evident from the harmonic output shown in Figure 4.21 and Figure 4.22. In the presence of a reactive power change, the steady-state current waveforms do not have a significant change in magnitude as the D-Q theory compensates for the reactive power of the system.

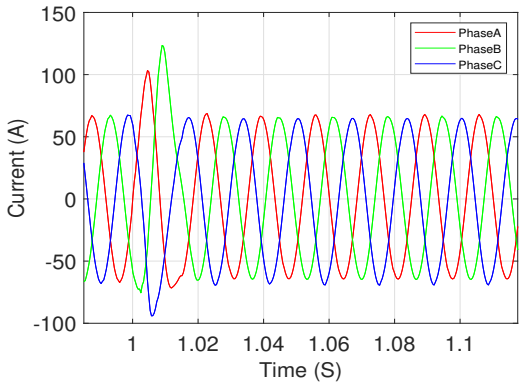

Figure 4.15: $TDHD_1$ Reactive Load Increase

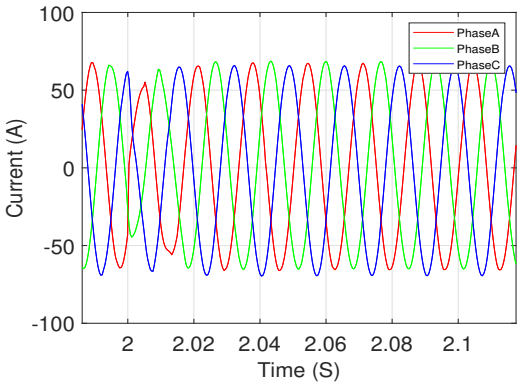

Figure 4.16: $TDHD_1$ Reactive Load Decrease

For $TDHD_2$, the settling time is again higher when compared to $TDHD_1$. For both the load addition (Figure 4.17) and load shredding (Figure 4.18) the settling time response are 0.10 s and 0.11 s. The TDD is measured 0.34% after reactive load increase and 0.32% after reactive load is shredded. The two TDHD provide reactive power compensation as Park's transformation has been implemented in $TDHD_1$ and $TDHD_2$. The transformation matrix can separate the active and reactive components as shown in the equations of subsection 3.3.1, resulting in no change in the APF output prior to and after a reactive load change.

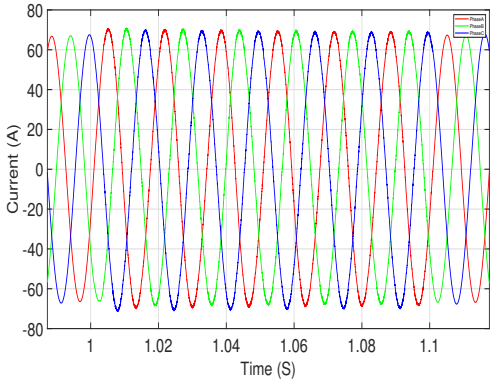

Figure 4.17: $TDHD_2$ Reactive Load Increase

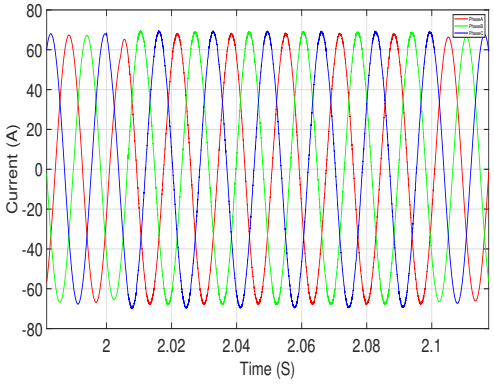

Figure 4.18: $TDHD_2$ Reactive Load Decrease

For the SDFT, the major difference is the current magnitude in response to a reactive load change. Figure 4.19 and Figure 4.20 illustrates that SDFT does not

have the capability to compensate the reactive power needs of the system which results in a different current magnitude after a reactive load change. This is a disadvantage if power factors are to be maintained. The TDD level is still good and is measured at 0.15% for both reactive load additions and load shredding. In this case the settling time is recorded at 0.08 s and 0.07 s for a reactive load increase and decrease, respectively.

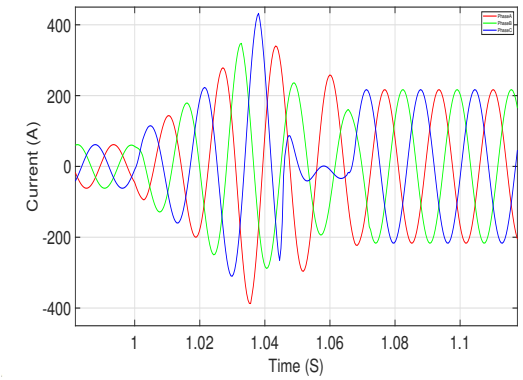

Figure 4.19: SDFT Reactive Load Increase

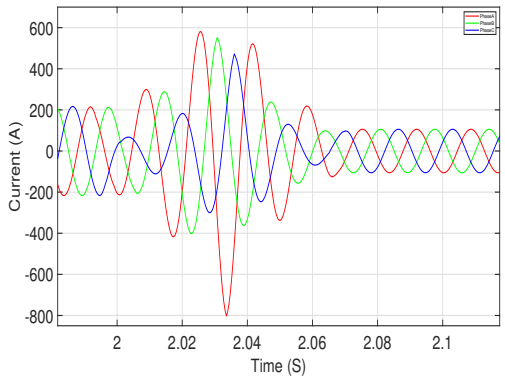

Figure 4.20: SDFT Reactive Load Decrease

For the reactive load fluctuation, $TDHD_2$ has the best performance among the three as illustrated in Figure 4.21 and Figure 4.22.

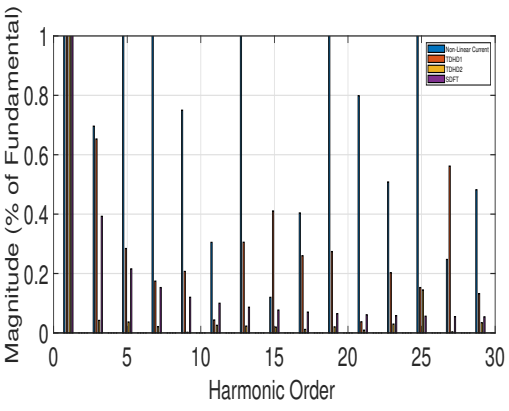

Figure 4.21: Harmonic Content for Reactive Load Increase

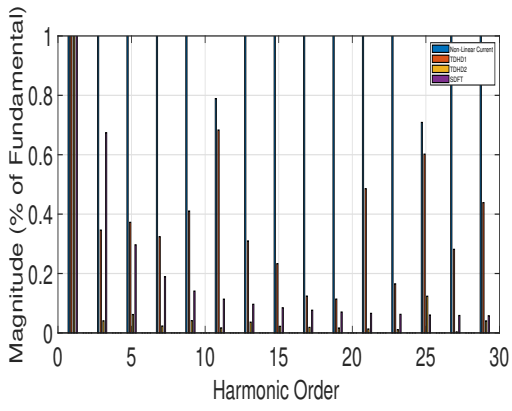

Figure 4.22: Harmonic Content for Reactive Load Decrease

4.4 Test Case 4: Non-Linear Load Change

In this test case, the non-linear load is increased to three times of the initial value of the Test Case 1, i.e. furnace heater operation during the winter and then replaced by a linear load of 40 kW. The objective of this test is to investigate how HD methods manage a step increase in non-linear load and then replaced with a linear load. Figure 4.23 and Figure 4.24 illustrates the test result for $TDHD_1$. For both the load changes, the settling time is 0.02 s. There is no significant overshoot in either case. TDD of 0.62% is measured after the non-linear is increased and 1.94% is recorded after the harmonic load is replaced by a linear load.

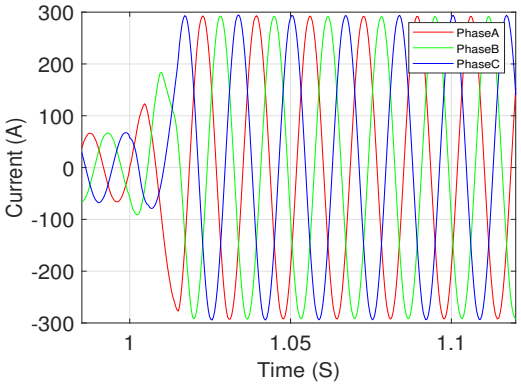

Figure 4.23: $TDHD_1$ Non-Linear Load Increase

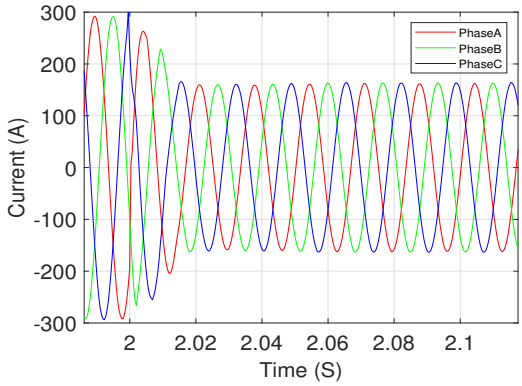

Figure 4.24: $TDHD_1$ Non-Linear Load Replacement

For the $TDHD_2$, the settling time is rounded to 0.10 s as shown in Figure 4.25. The steady-state current waveform for $TDHD_2$ has a lower TDD than $TDHD_1$ as found in the previous test setups. After the non-linear load has increased, the TDD is measured to be 0.41%. While after the linear load is added, a TDD of 0.36% is measured.

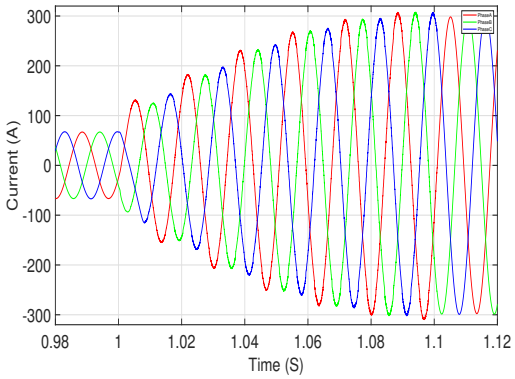

Figure 4.25: $TDHD_2$ Non-Linear Load Increase

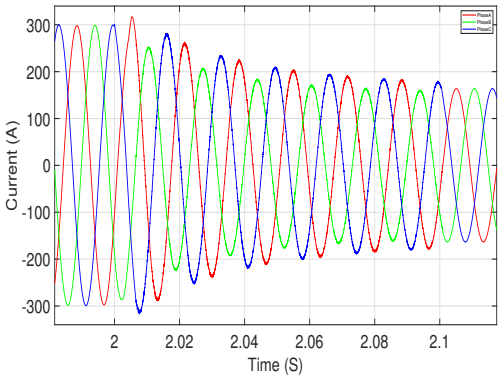

Figure 4.26: $TDHD_2$ Non-Linear Load Replacement

SDFT approach had the lowest TDD among the three HD algorithms. TDD levels of 0.18% is recorded for the addition of non-linear load. While after the non-linear load is replaced by the linear load, TDD is measured to be 0.20%. The settling time of 0.07 s is measured for the Figure 4.27 and Figure 4.28.

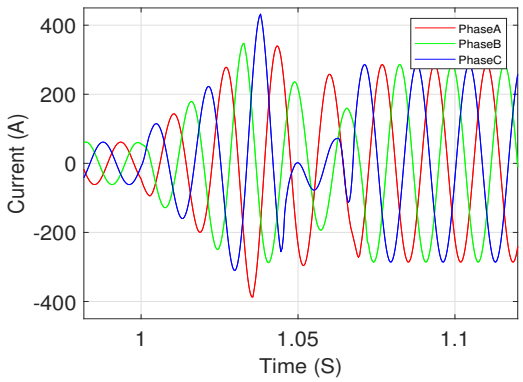

Figure 4.27: SDFT Non-Linear Load Increase

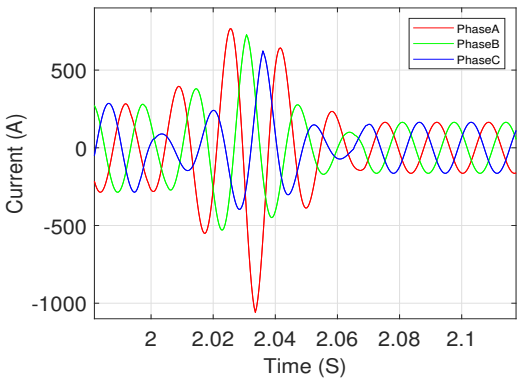

Figure 4.28: SDFT Non-Linear Load Replacement

The harmonic content for the three HD methods is shown in Figure 4.29 and Figure 4.30. The TDD level of the $TDHD_1$ is comparatively higher than the three HD methods utilized in this thesis. As the non-linear load is removed, the harmonic content from the load side has been significantly decreased. The test analysis shows even in the absence of the harmonic signals the APF will not disrupt the normal grid operation and is transparent in the output of the Figure 4.29 and Figure 4.30.

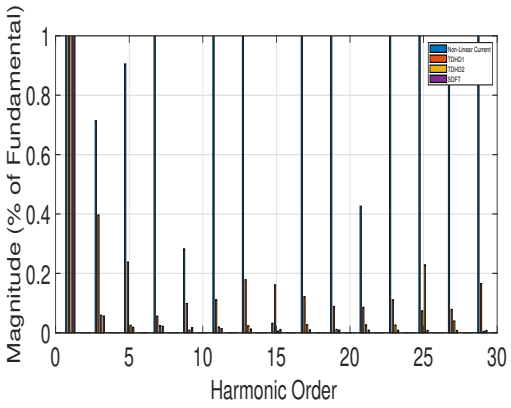

Figure 4.29: Harmonic Content for Non-Linear Load Increase

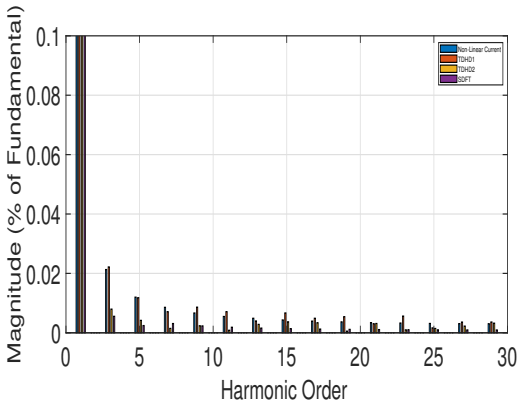

Figure 4.30: Harmonic Content for Non-Linear Load Replacement

4.5 Results Summary

From Table 4.1, all three HD methods show good TDD performance keeping levels well within the IEEE specified limits. Any APF using one of the three proposed HD methods can significantly reduce the line harmonic distortions in a wide differing harmonic conditions. $TDHD_2$ has the highest settling time to changing load conditions while the $TDHD_1$ method generally has the lowest. For the former, the distribution grid would be most affected by harmonics during the settling period.

The settling response of the SDFT output had the most overshoots as the DFT periodicity was disrupted with a load change but TDD and steady-state operation were very good. As $TDHD_2$ utilizes the Park's transformation for the fundamental current generation, a lower TDD than $TDHD_1$ was also expected. Table 4.1 shows the TDD performance for all test cases with SDFT showing a clear advantage for this performance metric.

Table 4.2 shows the settling time responses for all test cases. Settling time for $TDHD_2$ is comparatively higher than the other two HDs. A larger value of μ might have reduced the settling time, but overshoots can be seen even if the μ was set at maximum of $\frac{2}{\bar{\lambda}_{max}}$. A higher initial value of μ might result in a higher overshoot

which may have triggered the overcurrent relays.

Table 4.1: TDD Chart

Harmonic Detection Method	Test Case 1: Steady-State	Test Case 2: Active Load		Test Case 3: Reactive Load		Test Case 4: Non-Linear Load	
		Increase (kW)	Decrease (kW)	Increase (kVAR)	Decrease (kVAR)	Increase (kVA)	Decrease (kVA) to (kW)
$TDHD_1$	3.75	0.61	1.98	1.18	1.44	0.62	1.94
$TDHD_2$	1.32	0.33	0.32	0.34	0.32	0.41	0.36
SDFT	0.47	0.11	0.12	0.15	0.15	0.18	0.20
Load	47.84	7.92	11.79	57.46	78.63	29.53	1.82

Table 4.2: Settling Time Response

Harmonic Detection Method	Test Case 1: Steady-State	Test Case 2: Active Load		Test Case 3: Reactive Load		Test Case 4: Non-Linear Load	
		Increase (kW)	Decrease (kW)	Increase (kVAR)	Decrease (kVAR)	Increase (kVA)	Decrease (kVA) to (kW)
$TDHD_1$	0.01 s	0.06 s	0.07 s	0.025 s	0.02 s	0.02 s	0.02 s
$TDHD_2$	0.10 s	0.10 s	0.10 s	0.10 s	0.11 s	0.10 s	0.10 s
SDFT	0.004 s	0.08 s	0.08 s	0.08 s	0.07 s	0.07 s	0.07 s

From the harmonic plots of Figure 4.6, Figure 4.13, Figure 4.14, Figure 4.21, Figure 4.22, Figure 4.29, and Figure 4.30 no frequency shifting in the harmonic order can be observed. All the harmonic barplots are integer multiple of the fundamental order, which shows the absence of spectral leakage in the simulation. The waveshape distortion was prominent during the settling time response, but the fundamental frequency tracking capability through the use of the APF PLL ensures convergence. This also eliminates the Picket-Fence effects which would have been seriously jeopardize the SDFT implementation.

Finally, a fifth test case representing a three-phase fault was implemented in the SIMULINK setup. The simulation failed to converge the output current. The ODE45 (Runge-Kutta method) of SIMULINK may not be suitable to perform the fault analysis with the implemented HD methods.

Chapter 5

Conclusions and Future Work

5.1 Summary

This research has focused on active power filters to mitigate harmonic waveforms on a distribution grid. In this thesis, we simulate a modern distribution grid with residential non-linear loads and DER resources to instantiate the harmonic distortion. We present three HD techniques to be used in conjunction with a shunt configuration APF and assess its performance on based on various test scenarios. Two HD methods are based in the time domain, while the third utilizes the frequency domain. Settling response and TDD are measured under changing load and grid conditions to mimic the time-varying nature of the distribution systems.

This thesis implemented some modifications to improve HD performance with the adaptive LMS filtering method ($TDHD_2$) and the Fourier transformation method (SDFT). The established HD method, $TDHD_1$ was used as a reference for comparison purposes. The results demonstrated the effectiveness of the individual HD methods for four test cases used to model the day-to-day operation of a typical modern distribution system. Simulation results show $TDHD_2$ and SDFT having better TDD performance than $TDHD_1$, while $TDHD_2$ was found to have the slowest settling time after a load change. SDFT, which utilizes an efficient computation of the DFT using a sliding window, performed better than both TD methods in terms of TDD and had a very good settling time performance. This HD method, however, lacks the reactive power compensation scheme which can be clearly seen from the peaks of

the waveforms in the current axis of Figure 4.19 and Figure 4.20. Since our research focus was on harmonics compensation rather than the reactive power compensation, the SDFT algorithm would still be the overall recommendation of the HD technique to be implemented in the APF.

5.2 Future work

Since all of the results done in this research has been done on the simulation environment, future work is designed to include the following:

- ▷ The existing SIMULINK models can integrated with CYME to test the fault scenarios for the APF output.
- ▷ Develop a lab environment to represent the electrical characteristics of non-linear load and DER hardware-based simulators.
- ▷ Implement selected APFs with selected HD methods using current DSP hardware and electronic components.
- ▷ To verify the harmonic test outcomes using the lab equipment and APFs in a configured hardware setup.
- ▷ To model different DERs in the simulation setup, including wind and energy storage devices with weather dependent power variance to replicate the practical scenario.
- ▷ Incorporate demand response capabilities in the simulation. Demand response and power balancing for peak-shaving will certainly impact grid harmonics.

Bibliography

[1] J. Arrillaga, *Power System Harmonics*. New York: John Wiley & Sons, 1985.

[2] S. Czapp, "The effect of earth fault current harmonics on tripping of residual current devices," in *International School on Nonsinusoidal Currents and Compensation*, pp. 1–6, 2008.

[3] J. Phipps, J. Nelson, and P. Sen, "Power quality and harmonic distortion on distribution systems," *IEEE Transactions on Industry Applications*, vol. 30, no. 2, pp. 476–484, 1994.

[4] S. Santoso, H. W. Beaty, R. C. Dugan, and M. F. McGranaghan, *Electrical Power Systems Quality*. New York: McGraw-Hill, 1996.

[5] D. Thomas and M. Woolfson, "Evaluation of frequency tracking methods," *IEEE Transactions on Power Delivery*, vol. 16, no. 3, pp. 367–371, 2001.

[6] A. E. Emannuel, W. F. Horton, W. T. Jewel, and D. J. Phileggi, "Effects of Harmonics on Equipment Report of the IEEE Task Force on the Effects of Harmonics on Equipment," *IEEE Transaction on Power Delivery*, vol. 8, no. 2, 1993.

[7] E. Society, "IEEE Recommended Practice and Requirements for Harmonic Control in Electric Power Systems IEEE Power and Energy Society," *IEEE Std 519-2014 (Revision of IEEE Std 519-1992)*, vol. 2014, 2014.

[8] G. J. Wakileh, *Power Systems Harmonics: Fundamentals, Analysis and Filter Design*. Power Systems, Springer Berlin Heidelberg, 1st ed. ed., 2001.

[9] P. G. Cummings, "Estimating Effect of System Harmonics on Losses and Temperature Rise of Squirrel-Cage Motors," *IEEE Transactions on Industry Applications*, vol. 22, no. 6, pp. 1121–1126, 1986.

[10] B. H. Rudnick and J. Dixon, "Delivering Clean and Pure Power," *IEEE Power and Energy Magazine*, vol. 1, no. october, pp. 32–40, 2003.

[11] A. Fidigatti and E. Ragaini, "Effect of harmonic pollution on low voltage overcurrent protection," in *Proceedings of 14th International Conference on Harmonics and Quality of Power - ICHQP 2010*, pp. 1–4, 2010.

[12] S. Rechka, E. Ngandui, J. Xu, and P. Sicard, "Analysis of harmonic detection algorithms and their application to active power filters for harmonics compensation and resonance damping," *Canadian Journal of Electrical and Computer Engineering*, vol. 28, no. 1, pp. 41–51, 2003.

[13] H. Akagi, A. Nabae, and S. Atoh, "Control Strategy of Active Power Filters Using Multiple Voltage-Source Pwm Converters.," *IEEE Transactions on Industry Applications*, vol. IA-22, no. 3, pp. 460–465, 1986.

[14] G. Chang, C.-Y. Chen, and M.-C. Wu, "Measuring harmonics by an improved fft-based algorithm with considering frequency variations," in *IEEE International Symposium on Circuits and Systems (ISCAS)*, pp. 4 pp.–, 2006.

[15] W. S. Wood, F. P. Flynn, and A. Poray, "Effects of Supply Voltage Waveform Distortion on Motor Performance," in *International Conference on Sources and Effects of Power System Disturbances*, vol. 22, pp. 261–267, April 1974.

[16] L. Asiminoaei, F. Blaabjerg, and S. Hansen, "Evaluation of Harmonic Detection Methods for Active Power Filter Applications," in *Twentieth Annual IEEE Applied Power Electronics Conference and Exposition*, vol. 1, pp. 635–641, 2005.

[17] D. Chen and S. Xie, "Review of the control strategies applied to active power filters," in *2004 IEEE International Conference on Electric Utility Deregulation, Restructuring and Power Technologies. Proceedings*, vol. 2, pp. 666–670 Vol.2, 2004.

[18] K. Sozański, "Three phase active power filter with selective harmonics elimination," *Archives of Electrical Engineering*, vol. 65, no. 1, pp. 33–44, 2016.

[19] A. Massoud, S. Finney, and B. Williams, "Review of Harmonic Current Extraction Techniques for An Active Power Filter," in *11th International Conference on Harmonics and Quality of Power (IEEE Cat. No.04EX951)*, pp. 154–159, 2004.

[20] C. Lin, C. Chen, and C. Huang, "Calculating Approach and Implementation for Active Filters in Unbalanced Three-phase System using Synchronous Detection Method," in *Proceedings of the International Conference on Industrial Electronics, Control, Instrumentation, and Automation*, pp. 374–380 vol.1, 1992.

[21] N. Mendalek, K. Al-Haddad, L. Dessaint, and F. Fnaiech, "Nonlinear Control Strategy Applied to A Shunt Active Power Filter," in *IEEE 32nd Annual Power Electronics Specialists Conference (IEEE Cat. No.01CH37230)*, vol. 4, pp. 1877–1882, 2001.

[22] N. Mendalek and K. Al-Haddad, "Modeling and Nonlinear Control of Shunt Active Power Filter in The Synchronous Reference Frame," in *Ninth International Conference on Harmonics and Quality of Power. Proceedings (Cat. No.00EX441)*, vol. 1, pp. 30–35, 2000.

[23] S. Pigg and M. Bodson, "Adaptive Algorithms for The Rejection of Sinusoidal Disturbances Acting on Unknown Plants," *IEEE Transactions on Control Systems Technology*, vol. 18, no. 4, pp. 822–836, 2010.

[24] L. Qian, D. Cartes, H. Li, and L. Qi, "An Extended Adaptive Detection Method and Its Application in Power Quality Improvement," in *IEEE Power Engineering Society General Meeting*, pp. 1–6, 2007.

[25] L. Qian, D. Cartes, and H. Li, "Experimental Verification and Comparison of MAFC Method and D-Q Method for Selective Harmonic Detection," in *IECON 32nd Annual Conference on IEEE Industrial Electronics*, pp. 25–30, 2006.

[26] A. Girgis, W. Chang, and E. Makram, "A digital recursive measurement scheme for online tracking of power system harmonics," *IEEE Transactions on Power Delivery*, vol. 6, no. 3, pp. 1153–1160, 1991.

[27] H. Li, Y.-B. Li, Y.-P. Zou, and F. Liu, "Novel Adaptive Harmonic Detecting Algorithm Based on Variable Step-Size LMS," *Dianli Xitong Zidonghua(Autom. Electr. Power Syst.)*, vol. 29, no. 2, pp. 69–73, 2005.

[28] B. Widrow and S. D. Stearns, *Adaptive Signal Processing*. New Jersey: Prentice-Hall, 1985.

[29] N.-K. Nguyen, *"Approche neuromimétique pour l'identification et la commande des systèmes électriques : application au filtrage actif et aux actionneurs synchrones"*. PhD Thesis, Université de Haute Alsace - Mulhouse, Dec. 2010.

[30] F. C. De La Rosa, *Harmonics, power systems, and smart grids*. CRC Press, second edition ed., 2015.

[31] S. Clark, P. Famouri, and W. Cooley, "Elimination of supply harmonics," *IEEE Industry Applications Magazine*, vol. 3, no. 2, pp. 62–67, 1997.

[32] "Assumptions to the annual energy outlook 2014," *US Energy Information Administration*, pp. 1–197, 2014.

[33] D. Salles, C. Jiang, W. Xu, W. Freitas, and H. E. Mazin, "Assessing the Collective Harmonic Impact of Modern Residential Loads—Part I: Methodology," *IEEE Transactions on Power Delivery*, vol. 27, no. 4, pp. 1937–1946, 2012.

[34] C. Jiang, D. Salles, W. Xu, and W. Freitas, "Assessing the Collective Harmonic Impact of Modern Residential Loads—Part II: Applications," *IEEE Transactions on Power Delivery*, vol. 27, no. 4, pp. 1947–1955, 2012.

[35] D. Agrez, "Power system frequency estimation in the shortened measurement time," in *Proceedings of the 18th IEEE Instrumentation and Measurement Technology Conference. Rediscovering Measurement in the Age of Informatics (Cat. No.01CH 37188)*, vol. 2, pp. 1094–1098 vol.2, 2001.

[36] V. Wagner, J. Balda, D. Griffith, A. McEachern, T. Barnes, D. Hartmann, D. Phileggi, A. Emannuel, W. Horton, W. Reid, R. Ferraro, and W. Jewell, "Effects of Harmonics on Equipment," *IEEE Transactions on Power Delivery*, vol. 8, no. 2, pp. 672–680, 1993.

[37] A. E. Kennelly, F. A. Laws, and P. H. Pierce, "Experimental Researches On Skin Effect In Conductors," *Proceedings of the American Institute of Electrical Engineers*, vol. 34, no. 8, pp. 1749–1814, 1915.

[38] C. Erickson, "Motor Design Features For Adjustable-Frequency Drives," *IEEE Transactions on Industry Applications*, vol. 24, no. 2, pp. 192–198, 1988.

[39] E. Fuchs and M. A. S. Masoum, *Power Quality In Electrical Machines And Power Systems*. Academic Press, 2008.

[40] Y. G. Rebours, D. S. Kirschen, M. Trotignon, and S. Rossignol, "A survey of frequency and voltage control ancillary services—part i: Technical features," *IEEE Transactions on Power Systems*, vol. 22, no. 1, pp. 350–357, 2007.

[41] N. W. Miller, R. W. Delmerico, K. Kuruvilla, and M. Shao, "Frequency responsive controls for wind plants in grids with wind high penetration," in *IEEE Power and Energy Society General Meeting*, pp. 1–7, 2012.

[42] V. Akhmatov, H. Abildgaard, J. Pedersen, and P. Eriksen, "Integration of offshore wind power into the western danish power system," *Proc. Copenhagen Offshore Wind 2005*, 01 2005.

[43] Z. Gao, Y. Qiu, X. Zhou, and Y. Ma, "An overview on harmonic elimination," in *IEEE International Conference on Mechatronics and Automation (ICMA)*, pp. 11–16, 2015.

[44] G. W. Chang, H. J. Su, L. Y. Hsu, H. J. Lu, Y. R. Chang, Y. D. Lee, and C. C. Wu, "A study of passive harmonic filter planning for an ac microgrid," in *IEEE Power & Energy Society General Meeting*, pp. 1–4, 2015.

[45] I. E. Commission *et al.*, "Assessment of Emission Limits for Distorting Loads in MV and HV Power Systems," *IEC technical report*, vol. 61000, pp. 3–6, 1996.

[46] C. Cooper, "IEEE Recommended Practice for Electric Power Distribution for Industrial Plants," *Electron. Power*, vol. 33, no. 10, p. 658, 1987.

[47] Y. Sun, X. Xie, Q. Wang, L. Zhang, Y. Li, and Z. Jin, "A Bottom-Up Approach to Evaluate The Harmonics and Power of Home Appliances in Residential Areas," *Applied Energy*, vol. 259, p. 114207, 2020.

[48] H. E. Mazin, E. E. Nino, W. Xu, and J. Yong, "A Study on the Harmonic Contributions of Residential Loads," *IEEE Transactions on Power Delivery*, vol. 26, no. 3, pp. 1592–1599, 2011.

[49] C.-J. Chou, C.-W. Liu, J.-Y. Lee, and K.-D. Lee, "Optimal planning of large passive-harmonic-filters set at high voltage level," *IEEE Transactions on Power Systems*, vol. 15, no. 1, pp. 433–441, 2000.

[50] B. P. de Campos, L. A. de Sousa, and P. F. Ribeiro, "Mitigation of harmonic distortion with passive filters," in *17th International Conference on Harmonics and Quality of Power (ICHQP)*, pp. 646–651, 2016.

[51] L. Motta and N. Faúndes, "Active / passive harmonic filters: Applications, challenges amp; trends," in *17th International Conference on Harmonics and Quality of Power (ICHQP)*, pp. 657–662, 2016.

[52] N. Panmala and P. Sriyanyong, "Design and implementation of passive harmonic filter using simulation tool," in *2019 Research, Invention, and Innovation Congress (RI2C)*, pp. 1–5, 2019.

[53] M. Magraoui, *Validation de techniques de commande d'un filtre actif paralèlle*. PhD thesis, Ecole de Technologie Superieure, 2007.

[54] H. Akagi, "Active and Hybrid Filters for Power Conditioning," in *Proceedings of the IEEE International Symposium on Industrial Electronics (Cat. No.00TH8543)*, vol. 1, pp. 26–36, 2000.

[55] F. Peng, H. Akagi, and A. Nabae, "A New Approach to Harmonic Compensation in Power Systems-A Combined System of Shunt Passive and Series Active Filters," *IEEE Transactions on Industry Applications*, vol. 26, no. 6, pp. 983–990, 1990.

[56] H. Tokuda, I. Amano, and N. Eguchi, "A Resonance Dumping Control for A Line-Current Detection Type Active Filter," in *Proceedings of the Power Conversion Conference-Osaka (Cat. No.02TH8579)*, vol. 2, pp. 755–760 vol.2, 2002.

[57] F. Z. Peng, "Application Issues of Active Power Filters," *IEEE Industry Applications Magazine*, vol. 4, no. 5, pp. 21–30, 1998.

[58] Z. Salam, P. C. Tan, and A. Jusoh, "Harmonics mitigation using active power filter: A technological review," *Elektrika Journal of Electrical Engineering*, vol. 8, no. 2, pp. 17–26, 2006.

[59] H. Akagi, "New Trends in Active Filters for Improving Power Quality," in *Proceedings of the IEEE International Conference on Power Electronics, Drives & Energy Systems for Industrial Growth*, vol. 1, pp. 417–425, 1996.

[60] H. Fujita and H. Akagi, "The Unified Power Quality conditioner: The Integration of Series- and Shunt-Active Filters," *IEEE Transactions on Power Electronics*, vol. 13, no. 2, pp. 315–322, 1998.

[61] B. Singh, K. Al-Haddad, and A. Chandra, "A Review of Active Filters for Power Quality Improvement," *IEEE Transactions on Industrial Electronics*, vol. 46, no. 5, pp. 960–971, 1999.

[62] M. El-Habrouk and P. Darwish, M.K.and Mehta, "Active Power Filters: A Review," *IEE Proceddings-Electric Power Applications*, vol. 147, no. 5, pp. 403–413, 2000.

[63] L. Asiminoael, F. Blaabjerg, and S. Hansen, "Detection is key - harmonic detection methods for active power filter applications," *IEEE Industry Applications Magazine*, vol. 13, no. 4, pp. 22–33, 2007.

[64] S. Baig, F. ur Rehman, and M. Junaid Mughal, "Performance comparison of dft, discrete wavelet packet and wavelet transforms, in an ofdm transceiver for multipath fading channel," in *Pakistan Section Multitopic Conference*, pp. 1–6, 2005.

[65] G. Luzhnica, J. Simon, E. Lex, and V. Pammer, "A sliding window approach to natural hand gesture recognition using a custom data glove," in *IEEE Symposium on 3D User Interfaces (3DUI)*, pp. 81–90, 2016.

[66] A. A. Afridi, M. A. E. Ullah, and S. M. Hossain, "Harmonic reduction for non-linear loads using simulink based filter design," in *11th International Conference on Electrical and Computer Engineering (ICECE)*, pp. 459–462, 2020.

[67] N. H. Mendalek, *Quality of the electric wave and means of mitigation.* PhD thesis, Ecole de Technologie Superieure, 2003.

[68] A. Lopez, *ADVANCED CONTROLS FOR SYSTEMS DEDICATED TO IMPROVING THE QUALITY OF ENERGY: FROM LOW VOLTAGE TO TENSION UP.* PhD thesis, Institut National Polytechnique de Grenoble - INPG, 2006.

[69] K. Sergej, L. Asiminoaei, and S. Hansen, "Harmonic detection methods of active filters for adjustable speed drive applications," in *13th European Conference on Power Electronics and Applications*, pp. 1–10, 2009.

[70] B. M. Han, B. Y. Bae, and S. J. Ovaska, "Reference Signal Generator for Active Power Filters Using Improved Adaptive Predictive Filter," *IEEE Transactions on Industrial Electronics*, vol. 52, no. 2, pp. 576–584, 2005.

[71] G. Escobar, P. Mattavelli, A. M. Stanković, A. A. Valdez, and J. Leyva-Ramos, "An Adaptive Control for UPS to Compensate Unbalance and Harmonic Distortion Using a Combined Capacitor/Load Current Sensing," *IEEE Transactions on Industrial Electronics*, vol. 54, no. 2, pp. 839–847, 2007.

[72] B. Singh and J. Solanki, "An implementation of An Adaptive Control Algorithm for A Three-Phase Shunt Active Filter," *IEEE Transactions on Industrial Electronics*, vol. 56, no. 8, pp. 2811–2820, 2009.

[73] B. Widrow, J. Glover, J. McCool, J. Kaunitz, C. Williams, R. Hearn, J. Zeidler, J. Eugene Dong, and R. Goodlin, "Adaptive noise cancelling: Principles and applications," *Proceedings of the IEEE*, vol. 63, no. 12, pp. 1692–1716, 1975.

[74] B. Singh, A. Chandra, and K. Al-Haddad, *Power quality: problems and mitigation techniques*. John Wiley & Sons, 2014.

[75] S. Devassy and B. Singh, "Implementation of solar photovoltaic system with universal active filtering capability," *IEEE Transactions on Industry Applications*, vol. 55, no. 4, pp. 3926–3934, 2019.

[76] R. R. Pereira, C. H. da Silva, L. E. B. da Silva, G. Lambert-Torres, and J. O. P. Pinto, "New strategies for application of adaptive filters in active power filters," *IEEE Transactions on Industry Applications*, vol. 47, no. 3, pp. 1136–1141, 2011.

[77] X. Guo, H. Jiang, D. Zheng, W. Cong, and S. Jiang, "Harmonic Current Adaptive Predictable Based on Variable Step Size LMS Algorithm Used in APF," in *Proceedings of the 32nd Chinese Control and Decision Conference*, pp. 3289–3293, 2020.

[78] R. H. Kwong and E. W. Johnston, "A Variable Step Size LMS Algorithm," *IEEE Transactions on signal processing*, vol. 40, no. 7, pp. 1633–1642, 1992.

[79] D. K. M. John G. Proakis, *Digital Signal Processing*. Pearson, 4th ed., 2007.

[80] A. A. Girgis and F. M. Ham, "A Quantitative Study of Pitfalls in the FFT," *IEEE Transactions on Aerospace and Electronic Systems*, vol. AES-16, no. 4, pp. 434–439, 1980.

[81] S. H. Fathi, M. Pishvaei, and G. B. Gharehpetian, "A Frequency Domain Method for Instantaneous Determination of Reference Current in Shunt Active Filter," in *IEEE Region 10 Annual International Conference, Proceedings/TENCON*, pp. 14–17, 2006.

[82] E. Jacobsen and R. Lyons, "An Update to The Sliding DFT," *IEEE Signal Processing Magazine*, vol. 21, no. 1, pp. 110–111, 2005.

[83] T. Springer, "13 – sliding fft computes frequency spectra in real time," *Edn*, vol. 33, pp. 161–166, 1988.

[84] E. Jacobsen and R. Lyons, "The Sliding DFT," *IEEE Signal Processing Magazine*, vol. 20, no. 2, pp. 74–80, 2003.

[85] K. Sozanski, "Harmonic Compensation Using The Sliding DFT Algorithm," in *IEEE 35th Annual Power Electronics Specialists Conference (IEEE Cat. No.04CH37551)*, vol. 6, pp. 4649–4653, 2004.

[86] K. Sozanski, "Sliding DFT Control Algorithm for Three-Phase Active Power Filter," in *Twenty-First Annual IEEE Applied Power Electronics Conference and Exposition*, pp. 1223–1229, 2006.

[87] K. Sozański and M. Klyta, "Control Algorithm for Active Power Filter with Improved Transient Performance," in *10th European Conference on Power Electronics and Applications*, 2003.

[88] S. Mariethoz and A. C. Rufer, "Open Loop and Closed Loop Spectral Frequency Active Filtering," *IEEE Transactions on Power Electronics*, vol. 17, no. 4, pp. 564–573, 2002.

[89] K. Sozanski, "Noncausal current predictor for active power filter," in *Nineteenth Annual IEEE Applied Power Electronics Conference and Exposition. APEC '04.*, vol. 3, pp. 1470–1474 Vol.3, 2004.

[90] N. S. Nise, *Control Systems Engineering*. Wiley, 6 ed., 2010.

[91] R. Day, "How many kwh does the average home use?," 2016.

[92] T. George and D. Bones, "Harmonic power flow determination using the fast fourier transform," *IEEE Transactions on Power Delivery*, vol. 6, no. 2, pp. 530–535, 1991.

[93] J. William D. Stevenson, *Elements of power system analysis*. McGraw-Hill, 4 ed.

Vita

Candidate's full name: Riashad Siddique

University attended: Shahjalal University of Science and Technology, B.Sc.E., 2015

Publications:

Tahmid Hassan Talukdar, Rishad Siddique,Mehedhi Hasan, Conference Presentation,"Study of single junction solar cell characteristics varying different parameters" *2015 International Conference on Electrical Engineering and Information Communication Technology (ICEEICT)*, Savar , Bangladesh, May 21-23, 2015